

The Color Differences of Kuiper Belt Objects in Resonance with Neptune

Scott S. Sheppard¹

ABSTRACT

The optical colors of 58 objects in mean motion resonance with Neptune were obtained. The various Neptune resonant populations were found to have significantly different surface color distributions. The 5:3 and 7:4 resonances have semi-major axes near the middle of the main Kuiper Belt and both are dominated by ultra-red material (spectral gradient: $S \gtrsim 25$). The 5:3 and 7:4 resonances have statistically the same color distribution as the low inclination “cold” classical belt. The inner 4:3 and distant 5:2 resonances have objects with mostly moderately red colors ($S \sim 15$), similar to the scattered and detached disk populations. The 2:1 resonance, which is near the outer edge of the main Kuiper Belt, has a large range of colors with similar numbers of moderately red and ultra-red objects at all inclinations. The 2:1 resonance was also found to have a very rare neutral colored object showing that the 2:1 resonance is really a mix of all object types. The inner 3:2 resonance, like the outer 2:1, has a large range of objects from neutral to ultra-red. The Neptune Trojans (1:1 resonance) are only slightly red ($S \sim 9$), similar to the Jupiter Trojans. The inner 5:4 resonance only has four objects with measured colors but shows equal numbers of ultra-red and moderately red objects. The 9:5, 12:5, 7:3, 3:1 and 11:3 resonances do not have reliable color distribution statistics since few objects have been observed in these resonances, though it appears noteworthy that all three of the measured 3:1 objects have only moderately red colors, similar to the 4:3 and 5:2 resonances. The different color distributions of objects in mean motion resonance with Neptune are likely a result from the disruption of the primordial Kuiper Belt from the scattering and migration of the giant planets. The few low inclination objects known in the outer 2:1 and 5:2 resonances are mostly only moderately red. This suggests if the 2:1 and 5:2 have a cold low inclination component, the objects likely had a significantly different origin than the ultra-red dominated cold components of the cold classical belt and 5:3 and 7:4 resonances.

¹Department of Terrestrial Magnetism, Carnegie Institution of Washington, 5241 Broad Branch Rd. NW, Washington, DC 20015, USA, sheppard@dtm.ciw.edu

Subject headings: Kuiper belt: general – Oort Cloud – comets: general – minor planets, asteroids: general – planets and satellites: formation

1. Introduction

There is still a debate as to where the objects in the Kuiper Belt came from. It is likely that objects that originally formed in the giant planet region currently reside in the Kuiper Belt along with objects that formed beyond the giant planets (Gomes et al. 2003; Levison and Morbidelli 2003; Levison et al. 2008; Walsh et al. 2011). These various origins for the Kuiper Belt objects (KBOs) are one of the explanations as to why the colors of the KBOs have been found to be so diverse (Luu and Jewitt 1996). The environmental conditions experienced by KBOs such as space weathering, cratering and fragmentation may also cause the surfaces of the KBOs to change over time. Thus the surface color of a particular KBO is likely a combination of its original formation location within the solar nebula and the environmental conditions the KBO has experienced over the age of the solar system.

Dynamically there appear to be three main types of KBOs. (1) Objects that have their perihelion near Neptune ($q \sim 25 - 35$ AU) and have large eccentricities ($e > 0.4$) are called scattered disk objects. The scattered disk was likely created through KBOs having strong dynamical interactions with Neptune (Duncan and Levison 1997; Duncan 2008; Gomes et al. 2008). The detached disk objects, like the scattered disk, have moderate to large eccentricities ($e > 0.25$) but with higher perihelia ($q \gtrsim 40$ AU) and are thus unlikely to have been scattered by Neptune in the current solar system configuration. Detached disk objects are likely just fossilized scattered disk objects from the time when Neptune was still migrating outwards (Gladman et al. 2002; Lykawka and Mukai 2006; Gomes et al. 2011). (2) Objects with semi-major axes $42 \lesssim a \lesssim 48$ AU with moderate to low eccentricities are considered to be in the main Kuiper Belt and are called classical KBOs. The classical objects are usually split into two sub-categories based on inclination (Brown 2001). Objects with inclination less than 5 to 10 degrees are called low inclination or “cold” classical KBOs while those with higher inclinations are considered the “hot” classical KBOs. The low inclination “cold” classicals are redder, smaller and more prevalent in equal-sized binaries than other populations (Tegler and Romanishin 2000; Levison and Stern 2001; Trujillo and Brown 2002; Stern 2002; Gulbis et al. 2006; Noll et al. 2008; Peixinho et al. 2008). Tegler and Romanishin (2000) suggest that redder objects are based on eccentricity and perihelion distance and not simply inclination, with redder objects having larger eccentricities and perihelia. We find there is no significant canonical hot classical population as almost all objects with inclinations above 10 degrees in the classical region have much larger eccentricities and lower perihelia than the

cold classicals. Thus the standard hot classical population is more like the scattered disk objects than classical objects. The cold classical population likely formed relatively nearby their current locations as indicative of their low inclinations and eccentricities. In contrast, the hot and scattered population were likely scattered and captured into their current orbits based on their highly disturbed inclinations and eccentricities (Batygin et al. 2011; Wolff et al. 2012; Dawson and Murray-Clay 2012).

(3) Resonant KBOs, the main focus of this work, are objects that are in mean motion resonance with Neptune (Figures 1 and 2: see Elliot et al. 2005, Lykawka and Mukai 2007 and Gladman et al. 2008 for definitions of the various mean motion resonances with Neptune and www.boulder.swri.edu/~buie/kbo/kbofollowup.html for an updated list of Neptune resonant objects kept by Marc Buie). Resonant objects were likely captured into their respective resonance from the outward migration of Neptune in the early solar system (Malhotra 1995; Chiang and Jordan 2002; Chiang et al. 2003; Hahn and Malhotra 2005; Murray-Clay and Chiang 2005; Levison et al. 2008). The resonances with sizable known populations are the Neptune Trojans (1:1), the resonances with semi-major axes interior to the main classical Kuiper Belt 5:4, 4:3 and 3:2 (called Plutinos because Pluto is in this resonance), the 5:3 and 7:4 which have semi-major axes within the main classical Kuiper Belt and the outer resonances with semi-major axes exterior to the main classical Kuiper Belt 2:1 (called the Twotinos), 7:3, 5:2, and 3:1.

Where the resonant objects originated and how the resonant objects came to reside where they are today is still unknown. The dynamical and physical properties of KBOs in resonance with Neptune are extremely valuable since these objects were likely captured into these resonances from the outward migration of Neptune. The various orbital and physical characteristics of the resonant objects will help constrain the migration and evolution of the planets. It is likely that the different resonances swept up or captured objects from different initial locations. One way to try to understand how the resonances became populated is to determine the physical characteristics of individual resonance objects and compare them to other populations of small solar system objects.

Were the ultra-red objects emplaced into the Kuiper Belt or did they form in-situ? One of the simplest ways to try and answer this question is to catalog the current locations of ultra-red objects ($S \gtrsim 25$: Jewitt 2002; Sheppard 2010). Ultra-red material is mostly associated with the dynamcially stable cold classical KBOs and possibly the Oort cloud (Tegler and Romanishin 2000; Trujillo and Brown 2002; Peixinho et al. 2008; Sheppard 2010). Ultra-red colors are likely created from material rich in very volatile ices and organics and is mostly only seen on objects kept far from the Sun (Jewitt 2002; Grundy 2009; Sheppard 2010; Brown et al. 2011; Merlin et al. 2012).

This work observed the various KBOs in mean motion resonance with Neptune for their surface colors in order to look for similarities and differences between the objects in resonances and other classes of small solar system objects. The 3:2 resonance objects have been well explored physically because they are relatively brighter objects as they are located near the inner edge of the Kuiper Belt. Thus past color data of the 3:2 resonance objects is used and the focus of the new observations presented in this work is on the colors of the objects in the little explored more distant heavily populated resonances such as the 5:4, 4:3, 5:3, 7:4, 2:1, 5:2 and 3:1 as well as a few lesser populated resonances and Neptune Trojans in the 1:1 resonance with Neptune.

2. Observations

All new Kuiper Belt object color measurements presented in this work are from observations using the Magellan 6.5 meter telescopes at Las Campanas, Chile. Table 1 shows the geometry of the observations for the 58 objects observed. One of three imaging cameras were used during the observations with a standard set of Sloan filters. All observations were calibrated to Southern Sloan standard star fields G158-100, PG1633+099 or DLS-1359-11 (Smith et al. 2005). The LDSS3 imager on the Magellan-Clay telescope was used on the nights of 26 August 2009, and 20 and 21 March 2010. LDSS3 is a CCD imager with one STA0500A 4064×4064 CCD and $15\mu\text{m}$ pixels. The field of view is about 8.3 arcminutes in diameter with a scale of 0.189 arcseconds per pixel. The IMACS camera on the Magellan-Baade telescope was used on the nights of 20-21 April, 18 August, 11-12 September 2010, 27-28 September 2011 and 23-25 March 2012. IMACS is a wide-field CCD imager that has eight 2048×4096 pixel CCDs with a pixel scale of 0.20 arcseconds per pixel. The eight CCDs are arranged in a box pattern with four above and four below and about 12 arcsecond gaps between chips. Only chip 2 of IMACS, which is just North and West of the camera center, was used in this analysis. The MegaCam imager on the Magellan-Clay telescope was used on the nights of 9-10 October 2010. MegaCam has 36 CCDs of 2048×4608 pixels each with a pixel scale of 0.08 arcseconds per pixel giving a total field-of-view of $24' \times 24'$. Only chip 23, near the center, was used in this analysis.

The data analysis was done in the same way as described in Sheppard (2010). Biases and dithered twilight and dome flats were used to reduce each image. Images were obtained through either the Sloan g' , r' or i' filter while the telescope was auto-guiding at sidereal rates using a nearby bright star. Exposure times were between 300 and 350 seconds. Filters were rotated after each observation to prevent a light curve from influencing the color calculations. To be able to directly compare our results with previous works the Sloan colors were converted

to the Johnson-Morgan-Cousins BVRI color system using transfer equations from Smith et al. (2002): $B = g' + 0.47(g' - r') + 0.17$; $V = g' - 0.55(g' - r') - 0.03$; $V - R = 0.59(g' - r') + 0.11$; $R - I = 1.00(r' - i') + 0.21$. These transformation equations from Sloan to the BVRI color system were shown in Sheppard (2010) to be good to within a hundredth of a magnitude by observing bright TNOs with well known BVRI colors with the Sloan filters. The Sloan photometric observations are shown in Table 2 (Figure 3) and the BVRI derived photometric results are shown in Table 3 (Figure 4) with the orbital information of the objects given in Table 4.

Photometry was performed by optimizing the signal-to-noise ratio of the faint small outer Solar System objects. Aperture correction photometry was done by using a small aperture on the TNOs (0."64 to 1" in radius) and both the same small aperture and a large aperture (2."24 to 3."6 in radius) on several nearby unsaturated bright field stars with similar Point Spread Functions (PSFs). The magnitude within the small aperture used for the TNOs was corrected by determining the correction from the small to the large aperture using the PSF of the field stars (cf. Tegler and Romanishin 2000; Jewitt and Luu 2001; Sheppard 2010).

3. Results and Discussion

The BVRI colors are shown by Neptune resonance membership in Table 3 and Figure 4 for the new observations presented in this work. BVRI results for the already well observed 3:2 resonance as well as the few known measurements of other resonance objects are shown in Figure 5. Ultra-red color ($S \gtrsim 25$) was coined by Jewitt (2002) and is defined here as the color 75 percent of all cold classical Kuiper belt objects have. Very-red ($S \gtrsim 20$) is defined as the 90 percentile of all object colors in the cold classical Kuiper belt (Table 5). The correlated broadband optical colors of TNOs in Figure 4 shows they have a nearly linear red slope in their optical colors. This near linear optical color slope has been confirmed through spectroscopy and correlation analysis on other TNOs (Doressoundiram et al. 2008). The spectral gradient, S , is the percent of reddening per 100 nm in wavelength. Following our earlier paper Sheppard (2010) we express the spectral gradient as $S(\lambda_2 > \lambda_1) = (F_{2,V} - F_{1,V})/(\lambda_2 - \lambda_1)$, where λ_1 and λ_2 are the central wavelengths of the two filters used for the calculation and $F_{1,V}$ and $F_{2,V}$ are the flux of the object in the two filters normalized to the V-band filter. To compute the spectral gradient of the observed objects in this work with the Sloan filters, we used the g' and i' measurements. The g' and i' filters have well-separated central wavelengths of 481.3 and 773.2 nm, respectively.

It is immediately clear from Table 3 and Figure 4 that the various Neptune mean

motion resonances have significantly different color distributions. Just looking at colors versus resonance occupation shows the Neptune Trojans are all just slightly red, similar to the Jupiter Trojans (Karlsson et al. 2009). The inner 4:3 and outer 5:2 Neptune resonances are mostly moderately red objects like found in the scattered disk (Hainaut and Delsanti 2002) and detached disk (Sheppard 2010). The middle 5:3 and 7:4 Neptune resonances are dominated by ultra-red objects like found in the low inclination cold classical belt (Tegler and Romanishin 2000; Trujillo and Brown 2002; Peixinho et al. 2008). The 3:2 and 2:1 Neptune resonances have a wide range of colors from neutral to ultra-red. Assuming the surface colors of KBOs are related to their formation location, it is likely the 3:2 and 2:1 Neptune resonances have a greater mix of objects from around the solar system than the other reservoirs above. The 5:4 and 12:5 Neptune resonances have few known objects, but both appear to have significant numbers of ultra-red objects. The 3:1 resonance, with only three measured objects, does not have any known ultra-red members.

3.1. Size of Resonance Objects

The two main variables that one may think could significantly bias the color of objects within a resonance are the object size (Table 3) and orbital inclination (Table 4). Except for the 3:2 resonance, almost all the objects in the other resonances have absolute magnitudes $m_R(1, 1, 0) \gtrsim 6$ (radii $\lesssim 100$ km assuming moderate albedos), and thus are significantly smaller than the dwarf planet sized objects in the Kuiper Belt (Sheppard et al. 2011). This means that even the largest resonance objects are unlikely to have atmospheres or be strongly differentiated (McKinnon et al. 2008; Lineweaver and Norman 2010). This small size is also below the point where high albedos become prominent as seen on the largest KBOs (Stansberry et al. 2008; Santos-Sanz et al. 2012). Size should also not be a significant factor in biasing the resonant color results as almost all objects observed in this work have similar absolute magnitudes ($m_R(1, 1, 0) \sim 7$ mags) independent of which Neptune resonance they are in (see Table 3). This is true for all resonances except maybe the largest objects in the 3:2 resonance. In the 3:2 resonance, of which Orcus, Pluto and Ixion are dwarf planet sized, Ixion and Orcus have very different colors. Orcus is very neutral in color while Ixion is very red (Doressoundiram et al. 2002; de Bergh et al. 2005; DeMeo et al. 2009). Because of the known atmosphere of Pluto and its ability to significantly alter the surface of an object (Stern and Trafton 2008), the color of Pluto is not used in this work.

3.2. Orbital Parameters and Colors of Objects

Inclination has been found to be important for classical KBOs as objects with inclinations less than about 5 to 10 degrees are dominated by ultra-red colors (Tegler and Romanishin 2000; Trujillo and Brown 2002; Stern 2002; Gulbis et al. 2006; Peixinho et al. 2008). Table 4 shows the orbital elements of the resonant KBOs observed in this work. Tables 2 and 3 also show inclinations arranged in ascending order for each resonance. Inclination appears to be of some importance in terms of the number of known objects in each resonance (Figure 6). There are many more known low inclination objects in the 5:4, 5:3 and 7:4 resonance populations with few known high inclination objects compared to the other resonances (see Table 5). These three resonances also have the highest fraction of very-red and ultra-red objects (Table 5).

The spectral gradients versus inclinations for Neptune resonant objects are shown in Figures 7 and 8. Even though the 5:3 and 7:4 have mostly low inclination objects, they also have ultra-red objects at high inclinations. These ultra-red, high inclination 5:3 and 7:4 resonant objects could have once been on low inclination orbits that were excited to higher inclinations through resonance pumping (Lykawka and Mukai 2005a,2005b; Volk and Malhotra 2011). The 5:4 only has very low inclination members with measured colors (Figure 8), but even with so few of them known, it appears to have a mix of colors and not be as dominated by ultra-red material as the 5:3 and 7:4 resonances (Table 5). In contrast, the 12:5 only has known high inclination members, of which both have ultra-red colors (Figure 8). The 3:1 has no ultra-red objects but all measured 3:1 objects are of high inclination (Figure 8).

The only non ultra-red objects in the 5:3 and 7:4 resonances have inclinations greater than about 10 degrees, suggesting 10 degrees is the place to distinguish between the low inclination cold classical and high inclination classical belt populations. All objects in the 5:3 and 7:4 resonances below about 10 degrees are ultra-red. More low inclination 4:3 and high inclination 5:3 and 7:4 resonant objects need to be found and measured for colors to determine how statistically significant inclination is. As of the time of this writing, the known numbers of objects at some inclinations are very low in these resonances. It seems that the 5:4 and 3:1 resonant objects may only occupy low and high inclination orbits, respectively.

Tegler and Romanishin (2000) suggest that high perihelion distance and low eccentricity are also important quantities for the ultra-red material in the classical Kuiper Belt. Figures 9 to 11 compare the spectral gradient of the resonance objects to their perihelion distances, eccentricities and semi-major axes. There are no obvious strong correlations, but there is a moderate correlation at about the 97% confidence level (Pearson coefficient of 0.28 with a sample of 58 objects) that resonant objects with high perihelion distances are redder

(Figure 9). These object color results versus the dynamics of the objects are similar to the cold classical object results for the location of ultra-red material. There is still a strong debate as to why objects with higher perihelia would have redder colors and thus likely different surface compositions than objects with lower perihelia. This color difference could be related to the retention and/or irradiation of very volatile ices such as Ammonia, Methane or Methanol at large heliocentric distances (Schaller and Brown 2007; Grundy 2009; Brown et al. 2011; Merlin et al. 2012). For example, Methane’s condensation temperature is around 40K, which in our Solar System happens around 48 AU (Youdin and Kenyon 2012). This is a similar distance as the cold classical Kuiper belt and 5:3 and 7:4 resonances.

4. Discussion

4.1. Resonant Colors Compared

To compare the various resonant color populations directly, the Kolmogorov-Smirnov test and Student’s t-test were calculated using the known color data (Student 1908; Kolmogorov 1933; Smirnov 1948). Figure 12 displays the data graphically while the results are shown in Table 6. The 5:3 and 7:4 resonances both have a very similar ultra-red color distribution and thus could be drawn from the same parent population. The 4:3 and 5:2 Neptune resonances also have similar color distributions, being mostly moderately red objects. It is possible that the 4:3 and 5:2 populations are from the same parent population. As shown in Table 6, the 5:3/7:4 resonant objects can be rejected as having the same common parent population as the 4:3/5:2 resonant objects at about the 99% confidence level, assuming the currently observed KBO colors are from the original formation location within the solar system. The 2:1 and 3:2 resonant colors both cover a much wider color distribution than the other resonances and could be drawn from the same parent population. The 2:1 and 3:2 seem to have a mix of object colors and may represent many different originally separate parent populations. The 3:2 also appears to have the only significant population of neutral colored objects within the resonant populations. The Neptune Trojans seem to be unique and do not appear to be drawn from the same parent population as any of the other Neptune resonances.

4.2. Resonant Colors Compared to Other KBO Classes

Figure 13 further compares the various resonant color populations to the main Kuiper Belt reservoirs defined in the introduction such as the cold classical Kuiper belt, scattered

disk and detached disk. As shown in Table 6, the ultra-red dominated 5:3 and 7:4 Neptune resonances appear to be drawn from the same parent population as the cold classical belt objects. This suggests that the 5:3 and 7:4 resonant objects are just a continuation of the cold classical Kuiper Belt. If true, high inclination objects may not be expected to be a significant fraction of the 5:3 and 7:4 populations, though some orbit inclination modification is expected for objects in and around the 5:3 and 7:4 resonances (Lykawka and Mukai 2005a,2005b; Volk and Malhotra 2011).

In contrast, the 4:3 and 5:2 resonances may have similar origins as the scattered disk, detached disk and/or high inclination classical belt objects based on colors. Though low number statistics, the 3:1 resonance is probably similar to the 4:3 and 5:2 resonances. A similar origin for the 4:3, 5:2 and 3:1 resonances would not only explain their similar colors but also these populations lack of low inclination members. The low number of ultra-red type objects in the 4:3, 5:2 and 3:1 suggest these objects might have once been much closer to the Sun, where as discussed in section 3.2, highly volatile ice rich ultra-red material on their surfaces could be destroyed. These objects could have been later scattered and captured into their current distant, mostly high inclination, resonant orbits.

4.3. Neptune’s Migration History

Lykawka and Mukai (2005b) determined that the 2:1 resonance should be more heavily populated than the 5:3 or 7:4 based on numerical simulations of objects in the classical belt and Neptune’s orbital history. Murray-Clay and Schlichting (2011) suggest the resonant populations should have a low inclination “cold” component to their populations if Neptune had a slow and smooth migration. One might also expect these resonant “cold” components to be dominated by ultra-red material like found in the cold classical Kuiper belt (24 of 26 objects or 92% are very red or redder in color, see Table 5). As discussed above and shown in Table 5, very red colors dominate the 5:3 and 7:4 resonances and this might also be true for the sparsely known inner 5:4 Neptune resonance. The inner 3:2 resonance may also show a cold component as this resonance has 8 of 13 (67%) known objects with low inclination as being very red or redder. Though this is statistically the same amount of very red material at higher inclinations in the 3:2 resonance, putting into question if the 3:2 has a true cold component or if the low inclination objects are just simply a continuation of the 3:2 resonance as a whole. High fractions of very red objects at low inclinations do not appear to be true in any of the outer resonances observed to date. The 2:1 and 5:2 Neptune resonances both have a few known objects below 10 degrees inclination and thus could have a cold component, but these low inclination objects are not preferentially ultra-red. On the

contrary, only 3 of the 11 (27%) objects known with inclinations less than 10 degrees in the 2:1 and 5:2 resonances have very-red or ultra-red colors. This small very red or redder fraction is also true for objects in the 2:1 and 5:2 resonances using the statistically smaller samples of objects with inclinations less than 8 and 5 degrees, 2 of 7 (29%) and 1 of 3 (33%), respectively. Because the cold classical objects are so dominated by very red material (92%, Table 5), simple probability statistics (for example, the probability of 2 of the 3 known outer resonant objects with inclination less than 5 degrees observed for colors having only moderately red color if drawn from the cold classical objects color distribution would be $2/26 \times 1/25$) give about a 3 sigma result that the low inclination objects observed in the 2:1 and 5:2 resonances have a less red color distribution than the cold classical Kuiper belt objects. This suggests if there is a cold component to the outer resonances, it is composed of different objects or that the objects had significantly different environmental histories than the cold components of the inner and middle resonances.

In the slow smooth migration model, the outer Neptune resonances would have swept gently through the cold classical Kuiper belt region. Assuming the cold classical objects were fully formed, the slow smooth migration model would predict that many of the ultra-red cold classicals would have been captured into these outer resonances during this time. Assuming the colors of objects captured into the outer resonances are the same today, the significant differences in the various resonant population colors and the small number of ultra-red objects in the low inclination populations of the outer resonances suggests Neptune did not experience a significant slow smooth migration phase. Neptune likely had a much more chaotic migration history with a large eccentricity just after formation and scattering allowing many various small bodies to be captured in the outer Neptune resonances (Levison et al 2008). The absence of any obvious cold component in the outer resonances also agrees with the Hahn and Malhotra (2005) result that Neptune migration likely occurred after the Kuiper Belt was already dynamically stirred-up.

If the 5:3 and 7:4 resonant populations share a common origin with objects in the cold classical belt, it is expected that the 5:3 and 7:4 should have a high number of equal-sized, ultra-red binaries. This is because the cold classical belt has been found to have a binary fraction of about $\sim 30\%$ while the other types of Kuiper Belt objects have only about a 5% binary fraction (Noll et al. 2008). To date, the only known ultra-red, equal-sized binary found outside of the cold classical belt is 2007 TY430 (Sheppard et al. 2012). 2007 TY430 likely became “stuck” in the 3:2 resonance population after escaping from the cold classical region (Lykawka and Mukai 2006).

5. Summary

Fifty-eight Neptune mean motion resonance objects were observed for their optical surface colors. The various Neptune mean motion resonances were found to have significantly different object surface color distributions. This indicates vastly different origins and evolutions for the objects in resonance with Neptune. Ultra-red color ($S \gtrsim 25$, $g'-i' \gtrsim 1.2$ mags, $B-I \gtrsim 2.2$ mags) is defined here as the color 75 percent of all cold classical Kuiper belt objects have. Very-red color ($S \gtrsim 20$) is defined as the 90 percentile of all object colors in the cold classical Kuiper belt.

1. The 5:3 and 7:4 Neptune resonances are composed of mostly ultra-red objects. The few known high inclination objects in these resonances are also ultra-red in color. The colors of the 5:3 and 7:4 resonant objects are statistically identical to the low inclination cold classical belt colors. Thus the 5:3 and 7:4 resonant objects are likely just an extension of the cold classical belt. If true, the 5:3 and 7:4 objects should have a significant number of ultra-red, equal sized binaries as have been found in the cold classical belt. The only non very-red colored objects in the 5:3 and 7:4 resonances all have inclinations near 10 degrees, suggesting this is the inclination region that separates the low inclination cold classical and high inclination classical belt populations.

2. The inner 4:3 and outer 5:2 Neptune resonances have few ultra-red objects and are composed of mostly moderately red objects. These two resonances, along with the sparsely sampled 3:1 Neptune resonance, appear to have a similar color distribution as the scattered disk (including the high inclination, moderate eccentricity classical objects) and detached disk. If these populations all have a similar origin, it would also explain the abundance of high inclination objects and lack of low inclination objects found in these three Neptune resonances.

3. In contrast to the narrow color distributions found for the above resonances, the 2:1 and 3:2 resonances have a very wide color distribution. This indicates these two resonances likely captured objects that formed in many different places within the solar system, assuming the colors are uniquely associated with origin radius.

4. The Neptune Trojans appear to be unique in surface color for outer solar system objects as these objects are only slightly red. They are very similar to the Jupiter Trojans in color.

5. There is a moderate correlation that the higher perihelion resonant objects have redder surfaces, but it is only significant at about the 97% confidence level.

6. If there are low inclination “cold” components of the inner 3:2 and 5:4 resonances,

they could be composed of a large fraction of ultra-red objects, like found for the middle 5:3 and 7:4 resonances. This is because there are many objects with low inclinations in the 3:2 and 5:4 with very red colors. With the limited color data to date, the outer 2:1 and 5:2 resonances do not show a high fraction of ultra-red objects at low inclinations. This suggests if there is a cold component in the outer resonances, the surfaces of the objects are different than the cold components of the middle Neptune resonances as well as the cold classicals. If true, this makes it unlikely Neptune had a significant slow smooth migration phase in its past since these outer resonances would be expected to have a significant cold component similar to the ultra-red objects in the cold classical Kuiper belt that the resonances would have swept through.

Acknowledgments

The author thanks C. Trujillo and S. Benecchi for helpful comments and suggestions while writing this manuscript. This paper includes data gathered with the 6.5 meter Magellan Telescopes located at Las Campanas Observatory, Chile. S. S. was partially supported by the National Aeronautics and Space Administration through the NASA Astrobiology Institute (NAI) under Cooperative Agreement No. NNA04CC09A issued to the Carnegie Institution of Washington.

REFERENCES

- Batygin, K., Brown, M. and Fraser, W. 2011, ApJ, 738, 13.
- Benecchi, S., Noll, K., Grundy, W., Buie, M., Stephens, D. and Levison, H. 2009, Icarus, 200, 292.
- Benecchi, S., Noll, K., Stephens, D., Grundy, W. and Rawlins, J. 2011, Icarus, 213, 693.
- Boehnhardt, H. et al. 2002, AA, 395, 297.
- Brown, M. 2001, AJ, 121, 2804.
- Brown, M., Schaller, E., and Fraser, W. 2011, 739, L60.
- Chiang, E. et al. 2003, AJ, 126, 675.
- Chiang, E. and Jordan, A. 2002, AJ, 124, 3430.
- Dawson, R. and Murray-Clay, R. 2012, ApJ, 750, 43.
- Delsanti, A., Boehnhardt, H., Barrera, L., Meech, K., Sekiguchi, T. and Hainaut, O. 2001, AA, 380, 347-358.

- DeMeo, F. et al. 2009, *AA*, 493, 283.
- Doressoundiram, A., Peixinho, N., de Bergh, C., Fornasier, S. et al. 2002, *AJ*, 124, 2279.
- Doressoundiram, A., Peixinho, N., Doucet, C., Mousis, O., Barucci, M. A., Petit, J. and Veillet, C. 2005, *Icarus*, 174, 90.
- Doressoundiram, A., Boehnhardt, H., Tegler, S. and Trujillo, C. 2008, in *The Solar System Beyond Neptune*, ed. M. Barucci, H. Boehnhardt, D. Cruikshank and A. Morbidelli (Tucson: Univ of Arizona Press), 91-104.
- de Bergh, C., Delsanti, A., Tozzi, G., Dotto, E., Doressoundiram, A. and Barucci, M. A., 2005, *AA*, 437, 1115.
- Doressoundiram, A. et al. 2007, *AJ*, 134, 2186.
- Duncan, M. and Levison, H. 1997, *Science*, 276, 1670-1672.
- Duncan, M. 2008, *Space Science Reviews*, 138, 109-126.
- Elliot, J., Kern, S., Clancy, K. et al. 2005, *AJ*, 129, 1117.
- Fornasier, S. et al. 2004, *AA*, 421, 353.
- Gladman, B., Holman, M., Grav, T., Kavelaars, J., Nicholson, P., Aksnes, K. and Petit, J. 2002, *Icarus*, 157, 269.
- Gladman, B., Marsden, B. and VanLaerhoven, C. 2008, in *The Solar System Beyond Neptune*, eds. M. Barucci, H. Boehnhardt, D. Cruikshank and A. Morbidelli (Tucson: Univ of Arizona Press), 43-57.
- Gomes, R. 2003, *Icarus*, 161, 404.
- Gomes, R., Fernandez, J., Gallardo, T. and Brunini, A. 2008, in *The Solar System Beyond Neptune*, eds. M. Barucci, H. Boehnhardt, D. Cruikshank and A. Morbidelli (Tucson: Univ of Arizona Press), 259-273.
- Gomes, R. 2011, *Icarus*, 215, 661.
- Grundy, W. 2009, *Icarus*, 199, 560.
- Gulbis, A., Elliot, J. and Kane, J. 2006, *Icarus*, 183, 168.
- Hahn, J. and Malhotra, R. 2005, *AJ*, 130, 2392.
- Hainaut, O. and Delsanti, A. 2002, *AA*, 389, 641.
- Jewitt, D. and Luu, J. 2001, *AJ*, 122, 2099.
- Jewitt, D. 2002, *Astron. J.*, 123, 1039-1049.
- Karlsson, O., Lagerkvist, C. and Davidsson, B. 2009, *Icarus*, 199, 106.

- Kolmogorov, A. 1933, *G. Inst. Ital. Attuari*, 4, 83.
- Levison, H. and Stern, S. A. 2001, *AJ*, 121, 1730.
- Levison, H. and Morbidelli, A. 2003, *Nature*, 426, 419.
- Levison, H., Morbidelli, A., Vanlaerhoven, C., Gomes, R. and Tsiganis, K. 2008, *Icarus*, 196, 258-273.
- Lineweaver, C. and Norman, M. 2010, arXiv:1004.1091.
- Luu, J. and Jewitt, D. 1996, *AJ*, 112, 2310.
- Lykawka, P. S. and Mukai, T. 2005a, *P&SS*, 53, 1175.
- Lykawka, P. S. and Mukai, T. 2005b, *EM&P*, 97, 107.
- Lykawka, P. S. and Mukai, T. 2006, *P&SS*, 54, 87.
- Lykawka, P. S., and Mukai, T. 2007, *Icarus*, 189, 213.
- Malhotra, R. 1995, *AJ*, 110, 420.
- McKinnon, W. B., Prialnik, D., Stern, S. A., Coradini, A. 2008, in *The Solar System Beyond Neptune*, eds. M. Barucci, H. Boehnhardt, D. Cruikshank and A. Morbidelli (Tucson: Univ of Arizona Press), 213-241.
- Merlin, F., Quirico, E., Barucci, M. and de Bergh, C. 2012, *AA*, 544, 20.
- Murray-Clay, R. and Chiang, E. 2005, *ApJ*, 619, 623.
- Murray-Clay, R. and Schlichting, H. 2011, *ApJ*, 730, 132.
- Noll, K., Grundy, W., Stephens, D., Levison, H. and Kern, S. 2008, *Icarus*, 194, 758.
- Peixinho, N., Boehnhardt, H., Belskaya, I., Doressoundiram, A., Barucci, M. and Delsanti, A. 2004, *Icarus*, 170, 153-166.
- Peixinho, N., Lacerda, P. and Jewitt, D. 2008, *AJ*, 136, 1837.
- Petit, J. et al. 2011, *AJ*, 142, 131.
- Romanishin, W., Tegler, S. and Consolmagno, G. 2010, *AJ*, 140, 29.
- Santos-Sanz, P., Ortiz, J., Barrera, L. and Boehnhardt, H. 2009, *AA*, 494, 693-706.
- Santos-Sanz, P., Lellouch, E., Fornasier, S. et al. 2012, *AA*, 541, 92.
- Schaller, E. and Brown, M. 2007, *ApJ*, 659, L61.
- Sheppard, S. and Trujillo, C. 2006, *Science*, 313, 511.
- Sheppard, S. 2010, *AJ*, 139, 1394.
- Sheppard, S., Udalski, A., Trujillo, C., Kubiak, M., Pietrzynski, G. et al. 2011, *AJ*, 142, 98.

- Sheppard, S., Ragozzine, D., Trujillo, C. 2012, *AJ*, 143, 58.
- Smirnov, N. 1948, *Annals of Mathematical Statistics*, 19, 279.
- Smith, J., et al. 2002, *AJ*, 123, 2121.
- Smith, J., Allam, S., Tucker, D. et al. 2005, *BAAS*, 37, 1379.
- Snodgrass, C., Carry, B., Dumas, C. and Hainaut, O. 2010, *AA*, 511, 72.
- Stern, S. A., 2002, *AJ*, 124, 2297.
- Stern, S. A. and Trafton, L. 2008, in *The Solar System Beyond Neptune*, ed. M. Barucci, H. Boehnhardt, D. Cruikshank and A. Morbidelli (Tucson: Univ of Arizona Press), 365-380.
- Stansberry, J., Grundy, W., Brown, M., Cruikshank, D., Spencer, J., Trilling, D. and Margot, J. 2008, in *The Solar System Beyond Neptune*, ed. M. Barucci, H. Boehnhardt, D. Cruikshank and A. Morbidelli (Tucson: Univ of Arizona Press), 161-179.
- Student, 1908, *Biometrika*, 6, 1-25.
- Tegler, S. and Romanishin, W. 1998, *Nature*, 392, 49.
- Tegler, S. and Romanishin, W. 2000, *Nature*, 407, 979.
- Tegler, S., Romanishin, W., and Consolmagno, S. 2003, *ApJ*, 599, L49.
- Trujillo, C. and Brown, M. 2002, *ApJ*, 566, L125.
- Walsh, K., Morbidelli, A., Raymond, S., O'Brien, D. and Mandell, A. 2011, *Nature*, 475, 206.
- Wolff, S., Dawson, R. and Murray-Clay, R. 2012, *ApJ*, 746, 171.
- Volk, K. and Malhotra, R. 2011, *ApJ*, 736, 11.
- Youdin, A. and Kenyon, S. 2012, arXiv1206.0738.

Table 1. Circumstances of the Observations

Name	UT Date	R (AU)	Δ (AU)	α (deg)	$EXP_{g'}$ (s)	$EXP_{r'}$ (s)	$EXP_{i'}$ (s)
(26375) 1999 DE ₉	2010 Apr 20.983	36.38	35.58	0.96	600	600	600
(38084) 1999 HB ₁₂	2010 Mar 21.177	33.16	32.32	0.97	600	600	600
(79969) 1999 CP ₁₃₃	2010 Mar 21.135	32.83	31.83	0.05	600	600	600
(79978) 1999 CC ₁₅₈	2010 Apr 21.066	44.36	44.00	1.21	1200	900	1200
(118378) 1999 HT ₁₁	2010 Apr 20.148	40.58	39.59	0.31	1050	700	1050
(119878) 2002 CY ₂₂₄	2010 Apr 21.028	37.21	36.80	1.42	750	750	750
(119956) 2002 PA ₁₄₉	2010 Oct 09.143	43.36	42.42	0.44	1050	600	1050
(119979) 2002 WC ₁₉	2010 Mar 20.997	42.40	42.66	1.30	600	600	600
(126154) 2001 YH ₁₄₀	2010 Mar 20.066	36.59	36.07	1.34	300	300	300
(126154) 2001 YH ₁₄₀	2010 Mar 21.065	36.59	36.09	1.35	300	300	300
(126619) 2002 CX ₁₅₄	2010 Apr 21.117	39.54	38.72	0.83	1050	1050	1050
(127871) 2003 FC ₁₂₈	2010 Mar 20.173	33.23	32.24	0.12	300	300	300
(127871) 2003 FC ₁₂₈	2010 Mar 21.163	33.23	32.24	0.14	300	300	300
(130391) 2000 JG ₈₁	2010 Mar 20.316	35.01	34.56	1.47	1200	900	1200
(131696) 2001 XT ₂₅₄	2012 Mar 24.008	35.96	35.44	1.37	1050	1050	1050
(131696) 2001 XT ₂₅₄	2012 Mar 25.007	35.96	35.46	1.38	350	350	350
(131697) 2001 XH ₂₅₅	2012 Mar 23.014	33.39	32.85	1.45	700	700	700
(131697) 2001 XH ₂₅₅	2012 Mar 24.055	33.39	32.87	1.47	350	000	350
(131697) 2001 XH ₂₅₅	2012 Mar 25.024	33.39	32.88	1.48	700	350	700
(135024) 2001 KO ₇₆	2010 Mar 20.187	44.97	44.35	1.01	1200	900	1200
(135571) 2002 GG ₃₂	2010 Mar 21.280	36.81	36.33	1.36	1200	700	1050
(136120) 2003 LG ₇	2010 Mar 20.362	34.02	33.72	1.61	1200	350	900
(136120) 2003 LG ₇	2010 Mar 21.392	34.02	33.70	1.60	1200	350	1200
(137295) 1999 RB ₂₁₆	2010 Oct 10.220	33.71	32.72	0.14	1050	1050	1050
(143685) 2003 SS ₃₁₇	2010 Sep 11.152	27.87	26.97	0.93	900	900	900
(143707) 2003 UY ₁₁₇	2010 Sep 11.333	32.75	32.02	1.25	700	700	700
(149349) 2002 VA ₁₃₁	2010 Oct 10.308	38.14	37.24	0.60	600	600	600
(160147) 2001 KN ₇₆	2010 Mar 20.280	40.19	39.51	1.06	900	900	900
(181871) 1999 CO ₁₅₃	2010 Apr 20.024	41.60	41.30	1.32	2000	1200	1750
(308379) 2005 RS ₄₃	2010 Aug 18.260	42.33	41.73	1.12	600	600	600

Table 1—Continued

Name	UT Date	R (AU)	Δ (AU)	α (deg)	$EXP_{g'}$ (s)	$EXP_{r'}$ (s)	$EXP_{i'}$ (s)
(308460) 2005 SC ₂₇₈	2010 Oct 10.272	33.85	32.85	0.20	600	600	600
1998 UU ₄₃	2010 Oct 09.364	36.20	35.45	1.00	1050	900	1050
1999 CX ₁₃₁	2010 Mar 20.126	40.63	39.82	0.83	1200	900	1200
1999 HG ₁₂	2010 Mar 21.233	41.49	40.71	0.87	1400	700	1050
2000 CQ ₁₀₄	2010 Mar 21.201	38.03	37.08	0.41	900	900	900
2000 QL ₂₅₁	2010 Oct 09.090	39.38	38.39	0.30	700	700	700
2000 QN ₂₅₁	2010 Aug 18.369	37.05	36.37	1.17	1750	1050	1400
2001 FQ ₁₈₅	2010 Mar 20.233	36.76	35.86	0.69	1400	700	1050
2001 QE ₂₉₈	2010 Aug 18.327	37.14	36.33	0.96	1050	700	1050
2001 UP ₁₈	2010 Aug 18.285	50.64	50.17	1.03	1050	700	1050
2001 XP ₂₅₄	2010 Mar 20.037	33.13	32.69	1.55	900	600	900
2001 XP ₂₅₄	2010 Mar 21.049	33.13	32.70	1.57	350	350	350
2001 XQ ₂₅₄	2010 Apr 19.977	31.07	31.08	1.85	1050	1050	1050
2002 GD ₃₂	2010 Apr 21.165	50.46	49.56	0.13	1050	700	1050
2002 GS ₃₂	2010 Mar 21.321	37.84	37.34	1.32	1200	700	1050
2002 VV ₁₃₀	2010 Oct 09.242	36.23	35.28	0.50	1050	700	1050
2003 QW ₁₁₁	2010 Oct 09.050	44.32	43.46	0.70	1050	700	1050
2003 YW ₁₇₉	2010 Mar 20.080	35.73	35.19	1.34	1200	900	1200
2004 EG ₉₆	2010 Apr 20.097	32.08	31.09	0.26	1350	700	1350
2004 HM ₇₉	2012 Mar 23.333	38.47	37.66	0.88	600	600	600
2004 HM ₇₉	2012 Mar 24.355	38.47	37.65	0.86	1200	700	900
2004 HO ₇₉	2012 Mar 23.380	39.94	39.44	1.25	700	700	700
2004 OQ ₁₅	2011 Sep 26.994	39.78	39.35	1.31	1200	700	1200
2004 OQ ₁₅	2011 Sep 27.997	39.78	39.37	1.32	350	350	350
2004 PW ₁₀₇	2010 Sep 11.099	38.46	37.46	0.22	1200	1200	1200
2004 PW ₁₀₇	2010 Sep 12.118	38.46	37.46	0.20	600	600	600
2004 TT ₃₅₇	2010 Oct 09.325	31.65	30.88	1.17	700	600	700
2004 TV ₃₅₇	2010 Oct 09.290	35.83	35.09	1.10	600	600	600
2004 TX ₃₅₇	2010 Oct 10.338	28.95	28.25	1.44	600	600	600
2005 CA ₇₉	2010 Mar 21.079	37.26	36.62	1.18	600	600	600

Table 1—Continued

Name	UT Date	R (AU)	Δ (AU)	α (deg)	EXP $_{g'}$ (s)	EXP $_{r'}$ (s)	EXP $_{i'}$ (s)
2005 ER ₃₁₈	2010 Mar 21.108	31.00	30.07	0.68	600	600	600
2005 SE ₂₇₈	2010 Sep 11.292	37.83	37.01	0.91	1200	900	900
2005 SE ₂₇₈	2010 Sep 12.271	37.83	37.00	0.89	350	350	350
2005 SF ₂₇₈	2010 Oct 10.355	36.00	35.10	0.70	600	600	600
2006 CJ ₆₉	2012 Mar 23.050	34.30	33.51	1.03	1750	1050	1400
2006 CJ ₆₉	2012 Mar 24.076	34.30	33.52	1.05	700	700	700
2006 CJ ₆₉	2012 Mar 25.050	34.30	33.53	1.07	700	350	700
2006 QJ ₁₈₁	2010 Sep 12.381	34.21	34.05	1.67	600	600	600
2006 RJ ₁₀₃	2009 Aug 26.306	30.50	29.90	1.55	900	900	900
2006 SG ₃₆₉	2010 Sep 11.366	30.25	29.66	1.57	350	350	350
2006 SG ₃₆₉	2010 Sep 12.335	30.25	29.65	1.55	1050	700	1050
2007 VL ₃₀₅	2009 Aug 26.342	28.14	27.69	1.86	600	600	600

Quantities are the heliocentric distance (R), geocentric distance (Δ) and phase angle (α). UT Date shows the year, month, and time of day at the start of the observations for each object on each night it was observed. The total exposure time in each filter (g', r', i') for each object on each night is given in the last three columns. Individual exposure times were 300 or 350 seconds and filters were rotated after each observation to prevent any rotational light curves from influencing the color calculations.

Table 2. New Sloan g',r',i' Optical Photometry

Name	$m_{r'}$ (mag)	i (deg)	S ^a	$g'-r'$ (mag)	$r'-i'$ (mag)	$g'-i'$ (mag)
1:1 Nept. Trojans						
2006 RJ ₁₀₃	22.51 ± 0.02	08.2	7.3 ± 4	0.62 ± 0.05	0.19 ± 0.04	0.81 ± 0.05
2007 VL ₃₀₅	22.85 ± 0.05	28.1	12.1 ± 5	0.58 ± 0.07	0.35 ± 0.06	0.93 ± 0.07
5:4						
(308460) 2005 SC ₂₇₈	22.22 ± 0.03	01.5	34.5 ± 3	1.07 ± 0.04	0.45 ± 0.03	1.51 ± 0.04
(127871) 2003 FC ₁₂₈	22.34 ± 0.02	02.4	35.6 ± 3	0.98 ± 0.02	0.53 ± 0.02	1.51 ± 0.03
(131697) 2001 XH ₂₅₅	23.61 ± 0.04	02.9	14.6 ± 4	0.64 ± 0.04	0.36 ± 0.06	1.01 ± 0.05
(79969) 1999 CP ₁₃₃	22.55 ± 0.02	03.2	7.5 ± 2	0.57 ± 0.03	0.24 ± 0.03	0.81 ± 0.03
4:3						
2004 HM ₇₉	23.41 ± 0.04	01.2	10.7 ± 4	0.61 ± 0.06	0.29 ± 0.06	0.88 ± 0.05
(143685) 2003 SS ₃₁₇	22.23 ± 0.02	05.9	27.2 ± 5	0.86 ± 0.05	0.46 ± 0.03	1.32 ± 0.06
1998 UU ₄₃	22.79 ± 0.03	09.6	16.0 ± 3	0.73 ± 0.04	0.32 ± 0.04	1.03 ± 0.05
2005 ER ₃₁₈	22.76 ± 0.03	10.4	10.6 ± 2	0.63 ± 0.03	0.27 ± 0.03	0.90 ± 0.03
2000 CQ ₁₀₄	23.82 ± 0.03	13.5	8.7 ± 3	0.62 ± 0.04	0.23 ± 0.04	0.85 ± 0.05
2004 TX ₃₅₇	23.35 ± 0.05	16.2	15.3 ± 3	0.77 ± 0.04	0.27 ± 0.03	1.04 ± 0.04
5:3						
2000 QN ₂₅₁	23.56 ± 0.05	00.3	22.8 ± 5	0.82 ± 0.06	0.40 ± 0.07	1.21 ± 0.07
2003 YW ₁₇₉	22.91 ± 0.03	02.4	29.7 ± 3	1.01 ± 0.04	0.40 ± 0.04	1.39 ± 0.03
2002 VV ₁₃₀	23.36 ± 0.02	02.4	32.5 ± 2	1.00 ± 0.02	0.46 ± 0.02	1.46 ± 0.02
2001 XP ₂₅₄	22.97 ± 0.02	02.6	24.1 ± 2	0.87 ± 0.03	0.39 ± 0.04	1.25 ± 0.03
2002 GS ₃₂	23.49 ± 0.03	04.3	26.2 ± 4	0.90 ± 0.04	0.41 ± 0.04	1.32 ± 0.05
2005 SE ₂₇₈	22.76 ± 0.04	06.9	31.8 ± 2	0.94 ± 0.04	0.49 ± 0.04	1.45 ± 0.03
(149349) 2002 VA ₁₃₁	22.48 ± 0.03	07.1	36.6 ± 3	1.11 ± 0.03	0.46 ± 0.03	1.57 ± 0.04
1999 CX ₁₃₁	23.22 ± 0.03	09.8	15.9 ± 2	0.75 ± 0.03	0.30 ± 0.03	1.05 ± 0.03
(126154) 2001 YH ₁₄₀	21.23 ± 0.05	11.1	16.2 ± 2	0.76 ± 0.02	0.30 ± 0.02	1.06 ± 0.02
2006 CJ ₆₉	22.90 ± 0.02	17.9	33.5 ± 4	1.00 ± 0.03	0.48 ± 0.02	1.46 ± 0.04

Table 2—Continued

Name	$m_{r'}$ (mag)	i (deg)	S ^a	$g'-r'$ (mag)	$r'-i'$ (mag)	$g'-i'$ (mag)
7:4						
(181871) 1999 CO ₁₅₃	23.23 ± 0.02	00.8	29.3 ± 2	1.07 ± 0.03	0.35 ± 0.03	1.42 ± 0.03
1999 HG ₁₂	23.71 ± 0.03	01.0	24.9 ± 3	0.81 ± 0.04	0.45 ± 0.03	1.26 ± 0.04
(135024) 2001 KO ₇₆	23.38 ± 0.03	02.2	29.8 ± 2	0.93 ± 0.03	0.46 ± 0.03	1.39 ± 0.03
(160147) 2001 KN ₇₆	22.88 ± 0.02	02.6	24.1 ± 2	0.83 ± 0.03	0.42 ± 0.03	1.25 ± 0.02
2003 QW ₁₁₁	23.42 ± 0.03	02.7	23.9 ± 3	0.85 ± 0.06	0.40 ± 0.04	1.20 ± 0.05
2004 PW ₁₀₇	23.67 ± 0.11	02.8	22.9 ± 9	0.93 ± 0.12	0.32 ± 0.13	1.24 ± 0.14
2001 QE ₂₉₈	23.32 ± 0.05	03.7	29.1 ± 5	0.98 ± 0.07	0.41 ± 0.06	1.38 ± 0.06
(119956) 2002 PA ₁₄₉	22.80 ± 0.02	04.1	24.0 ± 2	0.92 ± 0.02	0.35 ± 0.02	1.27 ± 0.02
(118378) 1999 HT ₁₁	23.09 ± 0.02	05.1	29.7 ± 2	0.94 ± 0.04	0.45 ± 0.03	1.39 ± 0.03
2004 OQ ₁₅	23.19 ± 0.04	09.7	8.6 ± 3	0.65 ± 0.05	0.20 ± 0.05	0.85 ± 0.05
2005 SF ₂₇₈	22.07 ± 0.03	13.3	32.7 ± 3	1.05 ± 0.04	0.43 ± 0.04	1.48 ± 0.04
9:5						
2002 GD ₃₂	23.11 ± 0.03	6.6	30.1 ± 2	0.91 ± 0.04	0.48 ± 0.04	1.39 ± 0.03
2:1 Twotinos						
2001 UP ₁₈	23.22 ± 0.04	01.2	16.0 ± 4	0.73 ± 0.04	0.32 ± 0.05	1.04 ± 0.05
2001 FQ ₁₈₅	23.30 ± 0.03	03.2	34.2 ± 2	0.96 ± 0.04	0.52 ± 0.04	1.48 ± 0.03
2000 QL ₂₅₁	22.72 ± 0.02	03.7	11.3 ± 2	0.65 ± 0.03	0.27 ± 0.03	0.91 ± 0.04
(119979) 2002 WC ₁₉	20.81 ± 0.01	09.2	28.4 ± 1	0.92 ± 0.01	0.44 ± 0.01	1.36 ± 0.01
2004 TV ₃₅₇	22.24 ± 0.02	09.7	00.4 ± 1	0.47 ± 0.02	0.13 ± 0.02	0.60 ± 0.02
(308379) 2005 RS ₄₃	21.39 ± 0.02	10.0	11.2 ± 2	0.66 ± 0.03	0.26 ± 0.03	0.92 ± 0.03
2005 CA ₇₉	20.83 ± 0.02	11.7	21.9 ± 2	0.90 ± 0.03	0.32 ± 0.03	1.22 ± 0.03
(137295) 1999 RB ₂₁₆	22.22 ± 0.04	12.7	18.0 ± 2	0.75 ± 0.03	0.35 ± 0.03	1.10 ± 0.03
2006 SG ₃₆₉	22.23 ± 0.02	13.6	26.0 ± 2	0.91 ± 0.04	0.40 ± 0.04	1.31 ± 0.03
2000 JG ₈₁	23.33 ± 0.03	23.5	10.9 ± 2	0.58 ± 0.04	0.32 ± 0.04	0.89 ± 0.04
7:3						
(131696) 2001 XT ₂₅₄	23.05 ± 0.03	00.5	7.9 ± 3	0.64 ± 0.04	0.19 ± 0.05	0.84 ± 0.04

Table 2—Continued

Name	$m_{r'}$ (mag)	i (deg)	S ^a	g'-r' (mag)	r'-i' (mag)	g'-i' (mag)
12:5						
(119878) 2002 CY ₂₂₄	21.85 ± 0.01	15.7	29.9 ± 3	0.96 ± 0.03	0.44 ± 0.03	1.39 ± 0.04
(79978) 1999 CC ₁₅₈	22.16 ± 0.03	18.8	23.4 ± 3	0.89 ± 0.03	0.36 ± 0.03	1.25 ± 0.04
5:2						
2004 HO ₇₉	23.33 ± 0.06	05.6	23.6 ± 8	0.75 ± 0.07	0.47 ± 0.08	1.22 ± 0.09
2001 XQ ₂₅₄	22.81 ± 0.03	07.1	11.0 ± 2	0.56 ± 0.03	0.34 ± 0.03	0.90 ± 0.04
(143707) 2003 UY ₁₁₇	20.90 ± 0.01	07.5	19.7 ± 1	0.76 ± 0.01	0.38 ± 0.01	1.14 ± 0.01
(26375) 1999 DE ₉	20.37 ± 0.02	07.6	18.4 ± 1	0.80 ± 0.02	0.32 ± 0.02	1.12 ± 0.02
2004 TT ₃₅₇	22.80 ± 0.04 ^b	09.0	14.3 ± 2	0.74 ± 0.03	0.27 ± 0.04	0.99 ± 0.04
(38084) 1999 HB ₁₂	22.16 ± 0.03	13.2	14.7 ± 1	0.69 ± 0.03	0.32 ± 0.03	1.01 ± 0.02
(135571) 2002 GG ₃₂	23.04 ± 0.02	14.7	33.9 ± 3	1.01 ± 0.03	0.48 ± 0.04	1.49 ± 0.04
2004 EG ₉₆	23.13 ± 0.04	16.2	11.6 ± 3	0.67 ± 0.05	0.26 ± 0.03	0.93 ± 0.05
3:1						
2006 QJ ₁₈₁	22.47 ± 0.04	20.0	14.0 ± 4	0.73 ± 0.06	0.27 ± 0.04	1.01 ± 0.06
(136120) 2003 LG ₇	23.85 ± 0.04	20.1	9.8 ± 5	0.55 ± 0.06	0.32 ± 0.05	0.85 ± 0.07
11:3						
(126619) 2002 CX ₁₅₄	23.46 ± 0.03	16.0	22.2 ± 4	0.79 ± 0.05	0.41 ± 0.05	1.18 ± 0.06

^aThe normalized Spectral gradient for the optical colors of the observed objects using the g' and i' measurements.

Table 3. BVRI Colors Derived Using Sloan Colors from this work

Name	m_R (mag)	i (deg)	$m_R(1, 1, 0)$ (mag)	$m_B - m_R$ (mag)	$m_V - m_R$ (mag)	$m_R - m_I$ (mag)
1:1 Nept. Trojans						
2006 RJ ₁₀₃	22.28 ± 0.02	08.2	7.24 ± 0.04	1.31 ± 0.06	0.48 ± 0.05	0.40 ± 0.04
2007 VL ₃₀₅	22.63 ± 0.05	28.1	7.87 ± 0.09	1.24 ± 0.08	0.45 ± 0.07	0.56 ± 0.06
5:4						
(308460) 2005 SC ₂₇₈	21.93 ± 0.03	01.5	6.67 ± 0.05	2.03 ± 0.05	0.74 ± 0.04	0.66 ± 0.03
(127871) 2003 FC ₁₂₈	22.06 ± 0.02	02.4	6.89 ± 0.03	1.89 ± 0.03	0.69 ± 0.02	0.74 ± 0.02
(131697) 2001 XH ₂₅₅	23.38 ± 0.04	02.9	7.94 ± 0.06	1.34 ± 0.06	0.49 ± 0.05	0.57 ± 0.06
(79969) 1999 CP ₁₃₃	22.33 ± 0.02	03.2	7.23 ± 0.03	1.23 ± 0.04	0.45 ± 0.03	0.45 ± 0.03
4:3						
2004 HM ₇₉	23.19 ± 0.04	01.2	7.24 ± 0.06	1.29 ± 0.07	0.47 ± 0.06	0.50 ± 0.06
(143685) 2003 SS ₃₁₇	21.97 ± 0.02	05.9	7.44 ± 0.04	1.70 ± 0.06	0.62 ± 0.05	0.67 ± 0.03
1998 UU ₄₃	22.55 ± 0.03	09.6	6.85 ± 0.05	1.49 ± 0.05	0.54 ± 0.04	0.53 ± 0.04
2005 ER ₃₁₈	22.53 ± 0.03	10.4	7.58 ± 0.05	1.32 ± 0.04	0.48 ± 0.03	0.48 ± 0.03
2000 CQ ₁₀₄	23.59 ± 0.03	13.5	7.78 ± 0.04	1.31 ± 0.05	0.48 ± 0.04	0.44 ± 0.04
2004 TX ₃₅₇	23.10 ± 0.05	16.2	8.31 ± 0.08	1.55 ± 0.05	0.56 ± 0.04	0.48 ± 0.03
5:3						
2000 QN ₂₅₁	23.31 ± 0.05	00.3	7.47 ± 0.08	1.63 ± 0.07	0.59 ± 0.06	0.61 ± 0.07
2003 YW ₁₇₉	22.63 ± 0.03	02.4	6.92 ± 0.05	1.94 ± 0.05	0.71 ± 0.04	0.61 ± 0.04
2002 VV ₁₃₀	23.08 ± 0.02	02.4	7.47 ± 0.03	1.92 ± 0.03	0.70 ± 0.02	0.67 ± 0.02
2001 XP ₂₅₄	22.71 ± 0.02	02.6	7.28 ± 0.05	1.71 ± 0.04	0.62 ± 0.03	0.60 ± 0.04
2002 GS ₃₂	23.22 ± 0.03	04.3	7.26 ± 0.05	1.76 ± 0.05	0.64 ± 0.04	0.62 ± 0.04
2005 SE ₂₇₈	22.49 ± 0.04	06.9	6.62 ± 0.07	1.82 ± 0.05	0.66 ± 0.04	0.70 ± 0.04
(149349) 2002 VA ₁₃₁	22.18 ± 0.03	07.1	6.33 ± 0.05	2.10 ± 0.03	0.77 ± 0.03	0.67 ± 0.03
1999 CX ₁₃₁	22.98 ± 0.03	09.8	6.80 ± 0.05	1.52 ± 0.03	0.55 ± 0.03	0.51 ± 0.03
(126154) 2001 YH ₁₄₀	20.98 ± 0.05	11.1	5.16 ± 0.08	1.53 ± 0.03	0.56 ± 0.02	0.51 ± 0.02
2006 CJ ₆₉	22.62 ± 0.02	17.9	7.15 ± 0.04	1.92 ± 0.04	0.70 ± 0.03	0.69 ± 0.02

Table 3—Continued

Name	m_R (mag)	i (deg)	$m_R(1, 1, 0)$ (mag)	$m_B - m_R$ (mag)	$m_V - m_R$ (mag)	$m_R - m_I$ (mag)
7:4						
(181871) 1999 CO ₁₅₃	22.94 ± 0.02	00.8	6.55 ± 0.04	2.03 ± 0.04	0.74 ± 0.03	0.56 ± 0.03
1999 HG ₁₂	23.46 ± 0.03	01.0	7.18 ± 0.05	1.61 ± 0.05	0.59 ± 0.04	0.66 ± 0.03
(135024) 2001 KO ₇₆	23.11 ± 0.03	02.2	6.45 ± 0.05	1.81 ± 0.04	0.66 ± 0.03	0.67 ± 0.03
(160147) 2001 KN ₇₆	22.62 ± 0.02	02.6	6.45 ± 0.04	1.65 ± 0.04	0.60 ± 0.03	0.63 ± 0.03
2003 QW ₁₁₁	23.16 ± 0.03	02.7	6.63 ± 0.05	1.68 ± 0.07	0.61 ± 0.06	0.61 ± 0.04
2004 PW ₁₀₇	23.40 ± 0.11	02.8	7.57 ± 0.20	1.81 ± 0.14	0.66 ± 0.12	0.53 ± 0.13
2001 QE ₂₉₈	23.04 ± 0.05	03.7	7.24 ± 0.08	1.89 ± 0.08	0.69 ± 0.07	0.62 ± 0.06
(119956) 2002 PA ₁₄₉	22.53 ± 0.02	04.1	6.14 ± 0.04	1.79 ± 0.02	0.65 ± 0.02	0.56 ± 0.02
(118378) 1999 HT ₁₁	22.82 ± 0.02	05.1	6.74 ± 0.03	1.82 ± 0.05	0.67 ± 0.04	0.66 ± 0.03
2004 OQ ₁₅	22.96 ± 0.04	09.7	6.77 ± 0.07	1.36 ± 0.06	0.49 ± 0.05	0.41 ± 0.05
2005 SF ₂₇₈	21.78 ± 0.03	13.3	6.16 ± 0.04	2.00 ± 0.05	0.73 ± 0.04	0.64 ± 0.04
9:5						
2002 GD ₃₂	22.84 ± 0.03	6.6	5.83 ± 0.04	1.78 ± 0.05	0.65 ± 0.04	0.69 ± 0.04
2:1 Twotinos						
2001 UP ₁₈	22.98 ± 0.04	01.2	5.79 ± 0.07	1.49 ± 0.05	0.54 ± 0.04	0.53 ± 0.05
2001 FQ ₁₈₅	23.03 ± 0.03	03.2	7.32 ± 0.05	1.86 ± 0.05	0.68 ± 0.04	0.73 ± 0.04
2000 QL ₂₅₁	22.49 ± 0.02	03.7	6.54 ± 0.03	1.36 ± 0.04	0.49 ± 0.03	0.48 ± 0.03
(119979) 2002 WC ₁₉	20.54 ± 0.01	09.2	4.05 ± 0.03	1.79 ± 0.02	0.65 ± 0.01	0.65 ± 0.01
2004 TV ₃₅₇	22.03 ± 0.02	09.7	6.36 ± 0.04	1.07 ± 0.02	0.39 ± 0.02	0.34 ± 0.02
(308379) 2005 RS ₄₃	21.16 ± 0.02	10.0	4.74 ± 0.04	1.37 ± 0.04	0.50 ± 0.03	0.47 ± 0.03
2005 CA ₇₉	20.56 ± 0.02	11.7	4.70 ± 0.04	1.76 ± 0.03	0.64 ± 0.03	0.53 ± 0.03
(137295) 1999 RB ₂₁₆	21.98 ± 0.04	12.7	6.75 ± 0.05	1.52 ± 0.04	0.55 ± 0.03	0.56 ± 0.03
2006 SG ₃₆₉	21.96 ± 0.02	13.6	6.95 ± 0.04	1.78 ± 0.05	0.65 ± 0.04	0.61 ± 0.04
2000 JG ₈₁	23.11 ± 0.03	23.5	7.57 ± 0.05	1.24 ± 0.05	0.45 ± 0.04	0.53 ± 0.04
7:3						
(131696) 2001 XT ₂₅₄	22.82 ± 0.03	00.5	7.07 ± 0.05	1.34 ± 0.05	0.49 ± 0.04	0.40 ± 0.05

Table 3—Continued

Name	m_R (mag)	i (deg)	$m_R(1, 1, 0)$ (mag)	$m_B - m_R$ (mag)	$m_V - m_R$ (mag)	$m_R - m_I$ (mag)
12:5						
(119878) 2002 CY ₂₂₄	21.58 ± 0.01	15.7	5.67 ± 0.03	1.86 ± 0.04	0.68 ± 0.03	0.65 ± 0.03
(79978) 1999 CC ₁₅₈	21.90 ± 0.03	18.8	5.25 ± 0.05	1.74 ± 0.04	0.64 ± 0.03	0.57 ± 0.03
5:2						
2004 HO ₇₉	23.09 ± 0.06	05.6	6.90 ± 0.09	1.52 ± 0.09	0.55 ± 0.07	0.68 ± 0.08
2001 XQ ₂₅₄	22.59 ± 0.03	07.1	7.37 ± 0.06	1.21 ± 0.04	0.44 ± 0.03	0.55 ± 0.03
(143707) 2003 UY ₁₁₇	20.65 ± 0.01	07.5	5.35 ± 0.03	1.53 ± 0.01	0.56 ± 0.01	0.59 ± 0.01
(26375) 1999 DE ₉	20.12 ± 0.02	07.6	4.40 ± 0.04	1.60 ± 0.02	0.58 ± 0.02	0.53 ± 0.02
2004 TT ₃₅₇	22.56 ± 0.04	09.0	7.42 ± 0.07	1.50 ± 0.04	0.55 ± 0.03	0.48 ± 0.04
(38084) 1999 HB ₁₂	21.92 ± 0.03	13.2	6.62 ± 0.05	1.42 ± 0.03	0.52 ± 0.03	0.53 ± 0.03
(135571) 2002 GG ₃₂	22.76 ± 0.02	14.7	6.91 ± 0.04	1.94 ± 0.03	0.71 ± 0.03	0.69 ± 0.04
2004 EG ₉₆	22.90 ± 0.04	16.2	7.86 ± 0.06	1.39 ± 0.06	0.51 ± 0.05	0.47 ± 0.03
3:1						
2006 QJ ₁₈₁	22.23 ± 0.04	20.0	6.63 ± 0.08	1.49 ± 0.07	0.54 ± 0.06	0.48 ± 0.04
(136120) 2003 LG ₇	23.63 ± 0.04	20.1	8.08 ± 0.08	1.20 ± 0.07	0.43 ± 0.06	0.53 ± 0.05
11:3						
(126619) 2002 CX ₁₅₄	23.21 ± 0.03	16.0	7.15 ± 0.05	1.58 ± 0.06	0.58 ± 0.05	0.62 ± 0.05

A few of the above objects have also had colors independently determined and are not shown here but in Figure 5. The colors reported elsewhere and found in this work are within the uncertainties of the various observations. 1998 UU43 has VRI from Benecchi et al. (2011), 1999 CX131 has VRI from Benecchi et al. (2011) and BVRI from Peixinho et al. (2004), 1999 CO153 has VR Benecchi et al. (2011) and BVR from Trujillo and Brown (2002), 2003 QW111 has VI from Benecchi et al. (2009), 1999 HT11 has BVR from Trujillo and Brown (2002), 2000 QL251 has VI from Benecchi et al. (2009), 2002 WC19 has VI from Benecchi et al. (2009), 1999 RB216 has BVRI from Boehnhardt

et al. (2002), 2000 JG81 has VRI from Benecchi et al. (2011), 2002 CY224 has BVRI from Santos-Sanz et al. (2009), 1999 CC158 has BVRI from Delsanti et al. (2001) and Doressoundiram et al. (2002), 1999 DE9 has many BVRI sources including Jewitt and Luu (2001) and Delsanti et al. (2001), 1999 HB12 has BVR from Trujillo and Brown (2002) and BVRI from Peixinho et al. (2004), and 2002 CX154 has BVRI from Santos-Sanz et al. (2009).

Table 4. Orbital Information for Observed Objects

Name	Type ^a	q (AU)	i (deg)	e	a (AU)
2006 RJ ₁₀₃	1:1	29.31	08.2	0.029	30.20
2007 VL ₃₀₅	1:1	28.13	28.1	0.069	30.20
(308460) 2005 SC ₂₇₈	5:4	32.59	01.5	0.069	35.01
(127871) 2003 FC ₁₂₈	5:4	31.89	02.4	0.086	34.90
(131697) 2001 XH ₂₅₅	5:4	32.40	02.9	0.074	35.01
(79969) 1999 CP ₁₃₃	5:4	31.93	03.2	0.083	34.84
2004 HM ₇₉	4:3	33.35	01.2	0.082	36.33
(143685) 2003 SS ₃₁₇	4:3	27.87	05.9	0.241	36.71
1998 UU ₄₃	4:3	31.96	09.6	0.129	36.68
2005 ER ₃₁₈	4:3	30.63	10.4	0.161	36.49
2000 CQ ₁₀₄	4:3	27.99	13.5	0.237	36.67
2004 TX ₃₅₇	4:3	28.87	16.2	0.217	36.85
2000 QN ₂₅₁	5:3	36.98	00.3	0.128	42.42
2003 YW ₁₇₉	5:3	35.69	02.4	0.156	42.29
2002 VV ₁₃₀	5:3	35.19	02.4	0.175	42.65
2001 XP ₂₅₄	5:3	33.04	02.6	0.220	42.38
2002 GS ₃₂	5:3	37.61	04.3	0.105	42.04
2005 SE ₂₇₈	5:3	37.68	06.9	0.115	42.59
(149349) 2002 VA ₁₃₁	5:3	32.25	07.1	0.243	42.57
1999 CX ₁₃₁	5:3	32.44	09.8	0.232	42.23
(126154) 2001 YH ₁₄₀	5:3	36.37	11.1	0.144	42.48
2006 CJ ₆₉	5:3	32.59	17.9	0.230	42.20
(181871) 1999 CO ₁₅₃	7:4	39.91	00.8	0.088	43.74
1999 HG ₁₂	7:4	36.76	01.0	0.154	43.44
(135024) 2001 KO ₇₆	7:4	38.62	02.2	0.112	43.50
(160147) 2001 KN ₇₆	7:4	39.83	02.6	0.085	43.53
2003 QW ₁₁₁	7:4	38.88	02.7	0.114	43.88
2004 PW ₁₀₇	7:4	37.96	02.8	0.137	43.97
2001 QE ₂₉₈	7:4	36.93	03.7	0.160	43.98
(119956) 2002 PA ₁₄₉	7:4	36.22	04.1	0.172	43.77

Table 4—Continued

Name	Type ^a	q (AU)	i (deg)	e	a (AU)
(118378) 1999 HT ₁₁	7:4	38.73	05.1	0.111	43.58
2004 OQ ₁₅	7:4	38.15	09.7	0.126	43.66
2005 SF ₂₇₈	7:4	35.54	13.3	0.193	44.07
2002 GD ₃₂	9:5	38.11	06.6	0.141	44.35
2001 UP ₁₈	2:1	44.64	01.2	0.070	48.01
2001 FQ ₁₈₅	2:1	36.75	03.2	0.226	47.48
2000 QL ₂₅₁	2:1	37.51	03.7	0.219	48.04
(119979) 2002 WC ₁₉	2:1	35.50	09.2	0.263	48.15
2004 TV ₃₅₇	2:1	34.52	09.7	0.283	48.13
(308379) 2005 RS ₄₃	2:1	38.46	10.0	0.200	48.10
2005 CA ₇₉	2:1	37.08	11.7	0.226	47.91
(137295) 1999 RB ₂₁₆	2:1	33.64	12.7	0.298	47.93
2006 SG ₃₆₉	2:1	30.15	13.6	0.376	48.28
(130391) 2000 JG ₈₁	2:1	34.15	23.5	0.277	47.25
(131696) 2001 XT ₂₅₄	7:3	35.90	00.5	0.324	53.14
(119878) 2002 CY ₂₂₄	12:5	35.21	15.7	0.348	53.99
(79978) 1999 CC ₁₅₈	12:5	38.99	18.8	0.278	54.04
2004 HO ₇₉	5:2	32.43	05.6	0.410	54.94
2001 XQ ₂₅₄	5:2	31.06	07.1	0.442	55.70
(143707) 2003 UY ₁₁₇	5:2	32.48	07.5	0.422	56.18
(26375) 1999 DE ₉	5:2	32.21	07.6	0.418	55.36
2004 TT ₃₅₇	5:2	31.49	09.0	0.438	56.03
(38084) 1999 HB ₁₂	5:2	32.56	13.2	0.411	55.31
(135571) 2002 GG ₃₂	5:2	35.84	14.7	0.349	55.04
2004 EG ₉₆	5:2	32.06	16.2	0.420	55.24
2006 QJ ₁₈₁	3:1	31.66	20.0	0.500	63.29
(136120) 2003 LG ₇	3:1	32.43	20.1	0.476	61.84
(126619) 2002 CX ₁₅₄	11:3	37.96	16.0	0.467	71.17

^aResonant membership is from the Minor Planet Center as well as Elliot et al. (2005), Gladman et al. (2008), Petit et al. (2011) and the updated version of Elliot et al. (2005) kept by Marc Buie at www.boulder.swri.edu/~buie/kbo/astrom.

Quantities are the perihelion distance (q), semi-major axis (a), eccentricity (e) and inclination (i). Data taken from the Minor Planet Center.

Table 5. Spectral Gradients of Various Reservoirs

Type	N	Very-Red ($S > 20$)	Ultra-Red ($S > 25$)	$i < 10$ (deg)	$i < 5$ (deg)	\bar{S}	Reference
1:1	6	0%	0%	67%	33%	9.3 ± 3	1,2
5:4	4	50%	50%	100%	100%	20 ± 10	1
4:3	6	17%	17%	50%	17%	14 ± 3	1
3:2	28	54%	32%	46%	25%	19 ± 15	3,4,5,6,7
5:3	10	80%	60%	80%	50%	28 ± 4	1
7:4	14	86%	50%	78%	57%	26 ± 3	1,7,11,12
2:1	12	50%	42%	42%	25%	20 ± 15	1,3
7:3	3	67%	67%	67%	33%	25 ± 10	1,7,9,10
5:2	14	21%	14%	57%	7%	17 ± 5	1,6,7,8,12,14
3:1	3	0%	0%	0%	0%	13 ± 2	1,8
Scattered KBOs	22	18%	18%	18%	0%	16 ± 4	8,10,11
Detached Disk	12	0%	0%	17%	8%	14 ± 3	8
Cold Classical	26	92%	75%	100%	100%	27 ± 3	3,10,15,16
Outer Classical	5	80%	40%	40%	40%	23 ± 3	8
Inner Oort Cloud	3	100%	67%	0%	0%	25 ± 2	8

N is the number of objects used in the statistics. S is the spectral gradient as defined in the text using known B or g' and I or i'-band photometry normalized to the V-band. Very-red is defined as $S > 20$, which is the spectral gradient that 90% of the cold classical objects are redder than. Ultra-red is defined as $S > 25$, which is the spectral gradient that 75% of the cold classical objects are redder than. The \pm on the average spectral gradient, \bar{S} , is not an error but displays the general range the type of objects span. Percent of inclinations less than 10 or 5 degrees are only for those objects that have known good color measurements.

References for TNO colors used in statistics: 1) This Work; 2) Sheppard and Trujillo (2006); 3) Tegler and Romanishin (2000); 4) Jewitt and Luu (2001); 5) Delsanti et al. (2001); 6) Doressoundiram et al. (2002); 7) Peixinho et al. (2004); 8) Sheppard (2010); 9) Luu and Jewitt (1996); 10) Trujillo and Brown (2002); 11) Boehnhardt et al. (2002); 12) Santos-Sanz et al. (2009); 13) Tegler et al. (2003); 14) Doressoundiram et al. (2005); 15) Peixinho et al. (2008); 16) Gulbis et al. (2006).

Table 6. T-test and Kolmogorov-Smirnov Color Test Results

Type 1 ^a	Type 2 ^a	N ^b	t-stat ^c	t-test ^d	D-stat ^e	K-S ^d
Both Types may be Drawn from the Same Parent Population:						
Cold Classical	7:4	40	1.79	56%	0.31	70%
Cold Classical	5:3	36	0.85	12%	0.36	76%
Scattered Disk	4:3	28	1.31	23%	0.27	19%
Scattered Disk	5:2	36	0.45	42%	0.27	52%
Scattered Disk	2:1	34	-0.18	75%	0.35	77%
Scattered Disk	3:2	50	-0.20	76%	0.35	93%
Detached Disk	Scattered Disk	34	2.02	69%	0.23	24%
Detached Disk	4:3	18	0.51	36%	0.33	33%
Detached Disk	5:2	26	-0.86	92%	0.43	86%
2:1	3:2	40	0.79	17%	0.20	16%
4:3	5:2	20	1.80	56%	0.36	45%
5:3	7:4	24	0.35	48%	0.33	53%
Reject Both Types Being Drawn from the Same Parent Population:						
Cold Classical	2:1	38	2.88	92%	0.46	96%
Scattered Disk	1:1	28	4.10	99.53%	0.68	98.78%
Cold Classical	3:2	54	3.96	99.45%	0.49	99.82%
Cold Classical	4:3	32	5.10	99.36%	0.79	99.84%
Scattered Disk	5:3	32	-2.50	99.82%	0.68	99.85%
Scattered Disk	7:4	36	-2.35	99.80%	0.70	99.98%
Cold Classical	5:2	40	5.32	99.96%	0.71	99.99%
Cold Classical	1:1	32	16.4	99.99%	1.00	99.99%
5:3 or 7:4	5:2 or 4:3	-	-	~ 99%	-	~ 98%
1:1	Any Other	-	-	~ 99%	-	~ 99%

^aThe dynamical groups being tested.

^bThe number of objects used in the test.

^cThe t-statistic from the t-test.

^dThe level of confidence that the two groups are not drawn from the same

parent population using the t-test or Kolmogorov-Smirnov (K-S) test.

^eThe D-statistic from the Kolmogorov-Smirnov test.

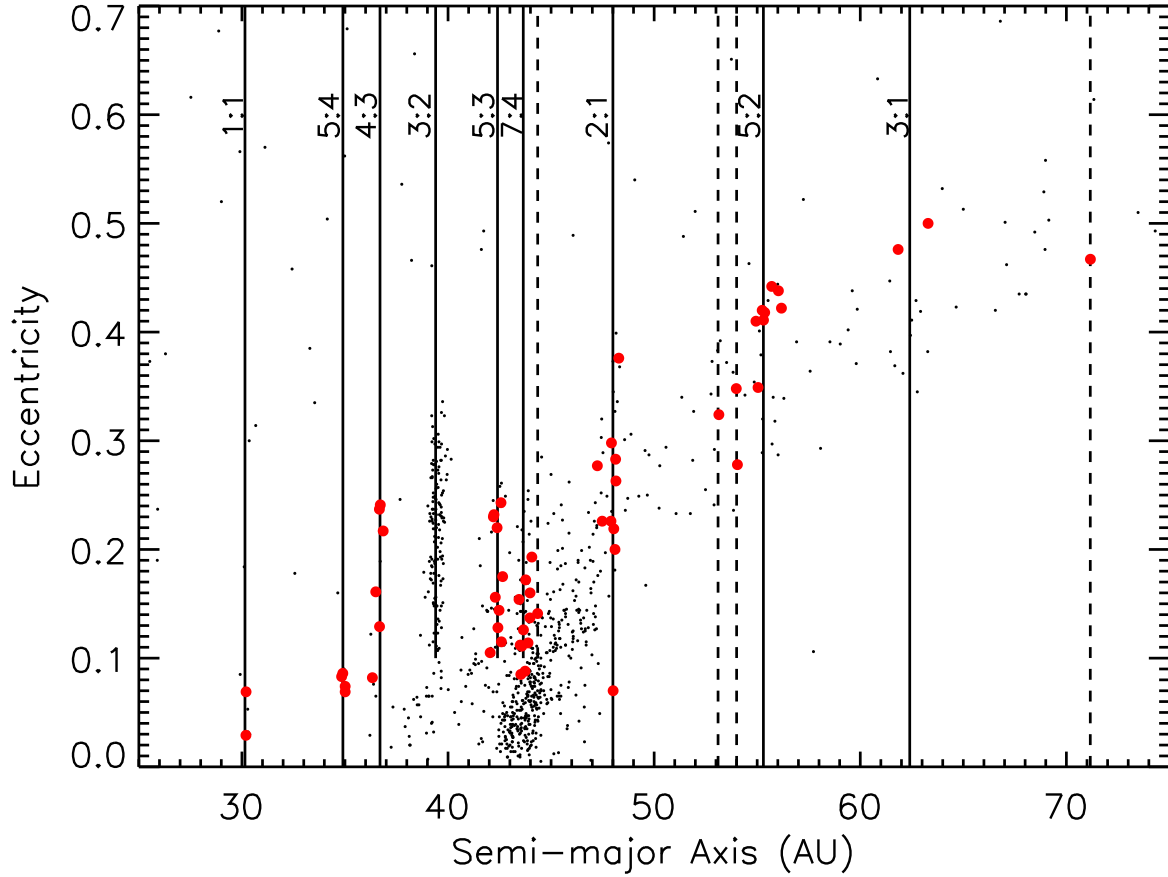


Fig. 1.— The semi-major axis versus eccentricity for all multi-opposition observed TNOs. Objects observed in this work are shown with big filled red circles. The main Neptune mean motion resonances are shown by vertical solid lines. The less important higher order resonances in which objects were observed in this work are shown with dashed lines (9:5, 7:3, 12:5, 11:3).

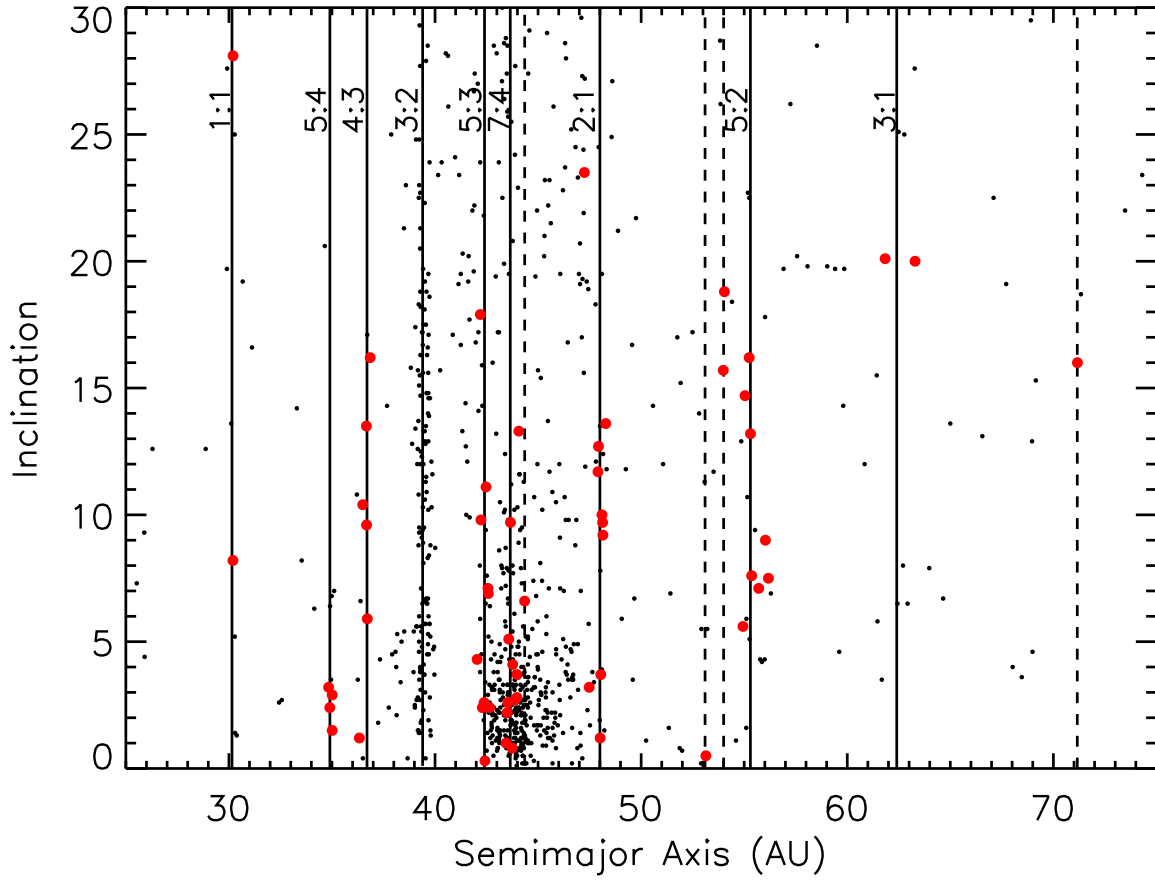


Fig. 2.— The semi-major axis versus inclination for all multi-opposition observed TNOs. Objects observed in this work are shown with big filled red circles.

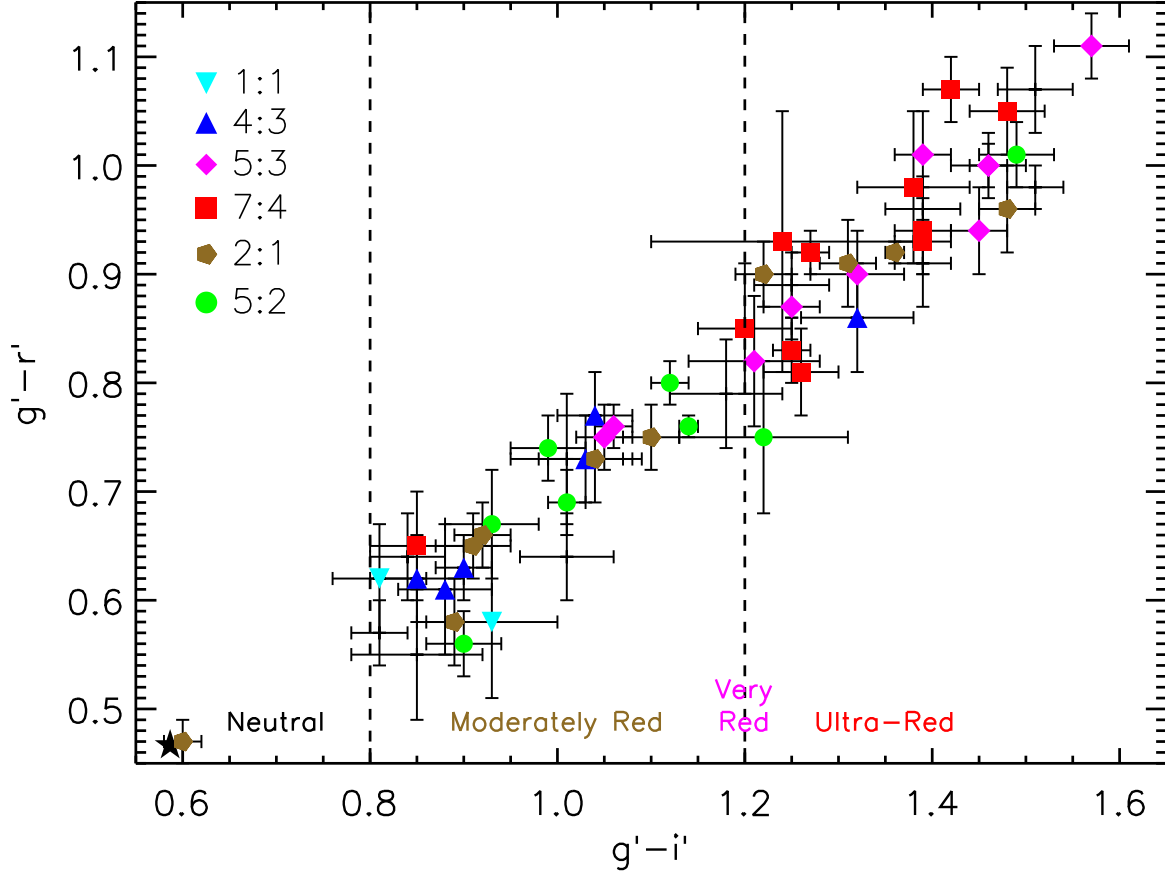


Fig. 3.— New Sloan g',r' and i' colors for Kuiper Belt objects observed in this work. The middle distance 5:3 (purple diamonds) and 7:4 (red squares) resonance populations appear mostly in the ultra-red portion of the figure (upper right) and are similar to the color of low inclination Classical Kuiper Belt objects. The inner 4:3 (blue triangles) and distant 5:2 (green circles) resonance populations are mostly only moderately red and similar to the colors of the comets, Jupiter Trojans and Neptune Trojans. The distant 2:1 appears to be a mix of neutral, moderately red and ultra-red objects (brown pentagons). Objects observed in this work in other resonances other than the main ones listed above are shown by plus signs. For reference the color of the Sun is marked by a filled black star. The ultra-red color is only seen on outer solar system objects and is defined here as the color 75% of the cold classical belt objects have. Very-red is defined as the color 90% of the cold classical belt objects have.

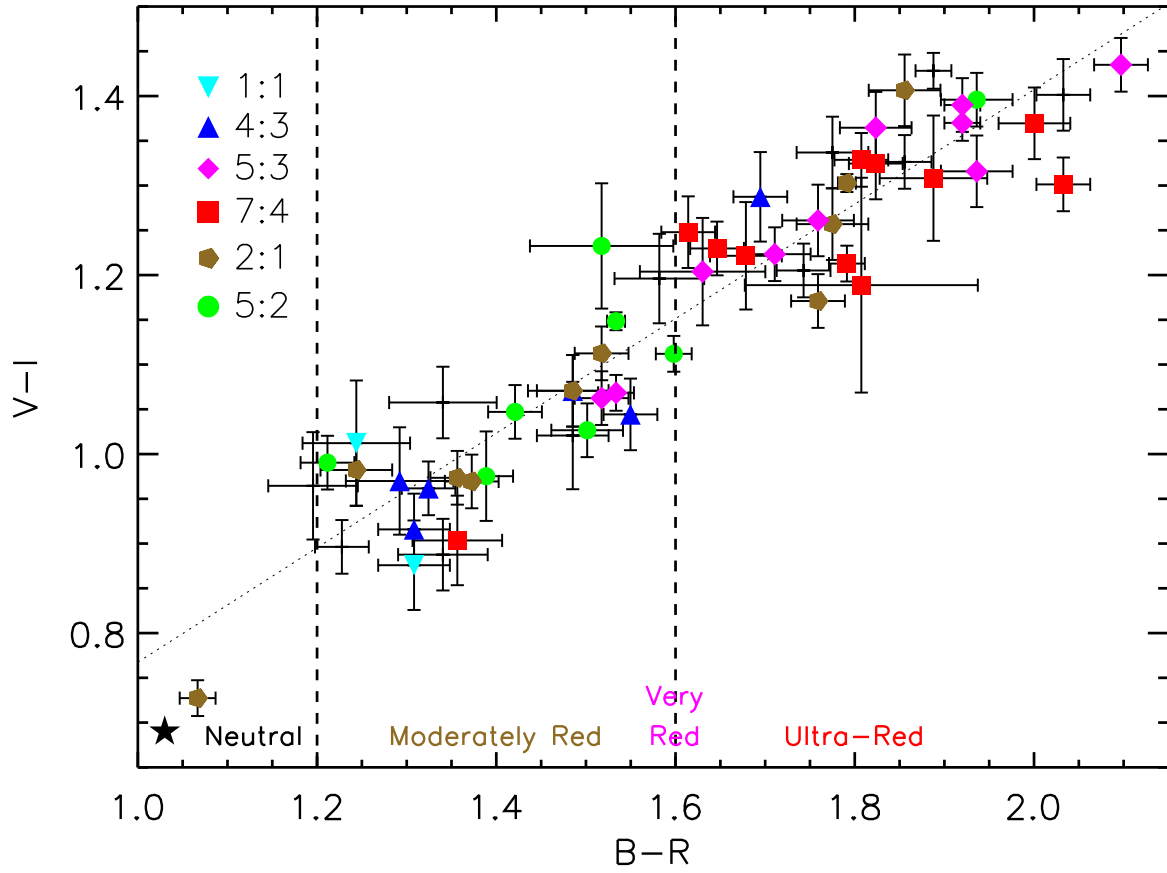


Fig. 4.— Same as Figure 3 except for BVRI colors $B-R$ and $V-I$ for objects observed in this work.

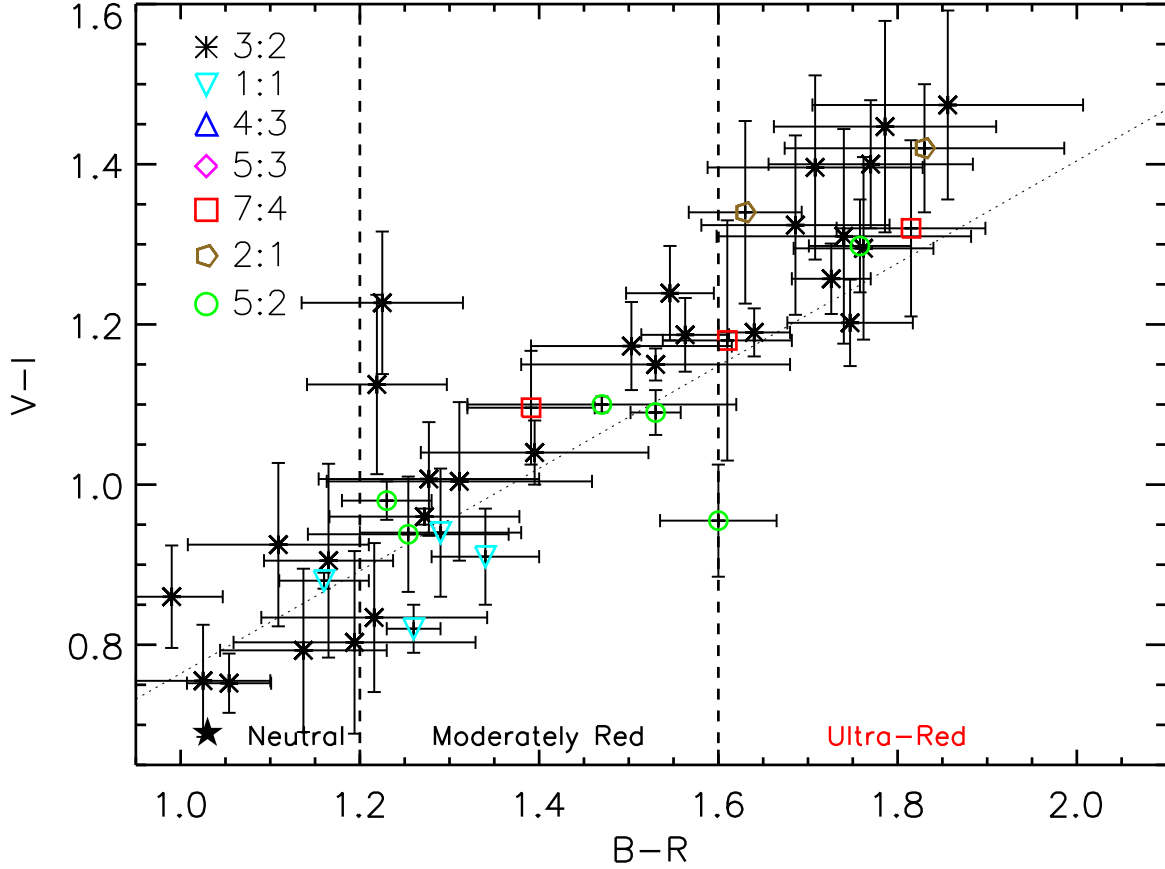


Fig. 5.— Previously measured BVRI colors of resonant Kuiper Belt objects not observed in this work. Very few resonant objects not in the 3:2 population have had previous good color measurements. Objects in the literature with error bars significantly larger than 0.1 magnitudes in color are not used. Data is from the MBOSS data base originally published in Hainaut and Delsanti (2002) as well as Luu and Jewitt (1996), Tegler and Romanishin (1998), Tegler and Romanishin (2000), Jewitt and Luu (2001), Delsanti et al. (2001), Doressoundiram et al. (2002), Tegler et al. (2003), Fornasier et al. (2004), Peixinho et al. (2004), Doressoundiram et al. (2005), Sheppard and Trujillo (2006), Doressoundiram et al. (2007), DeMeo et al. (2009), Santos-Sanz et al. (2009), Sheppard (2010), Snodgrass et al. (2010), Romanishin et al. (2010) and Benecchi et al. (2011).

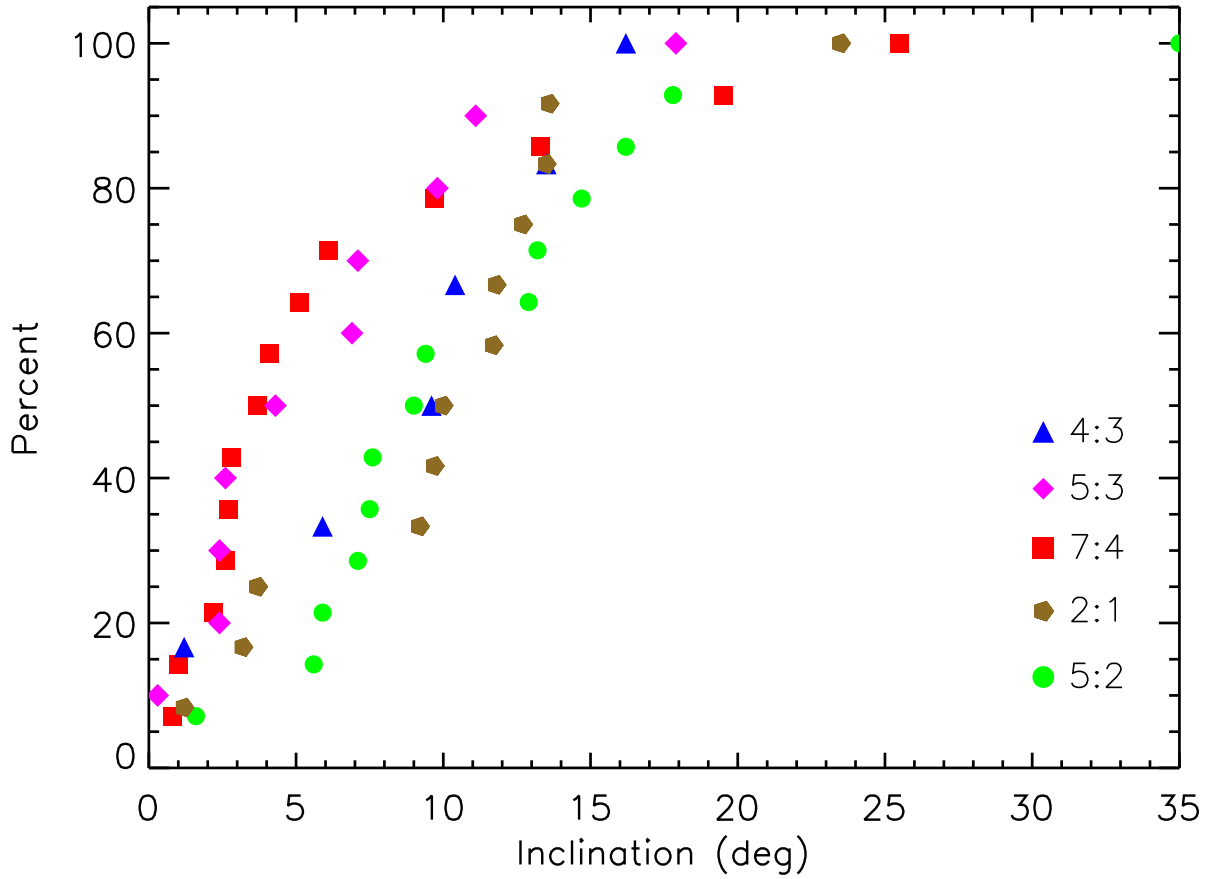


Fig. 6.— The orbital inclination versus percentage for the main Neptune resonances. The 5:3 and 7:4 resonances have more known low inclination objects than the other resonances. Thus the 5:3 and 7:4 are not only similar in ultra-red color as the Cold Classical belt objects but also have preferentially low inclinations like the Cold Classical belt.

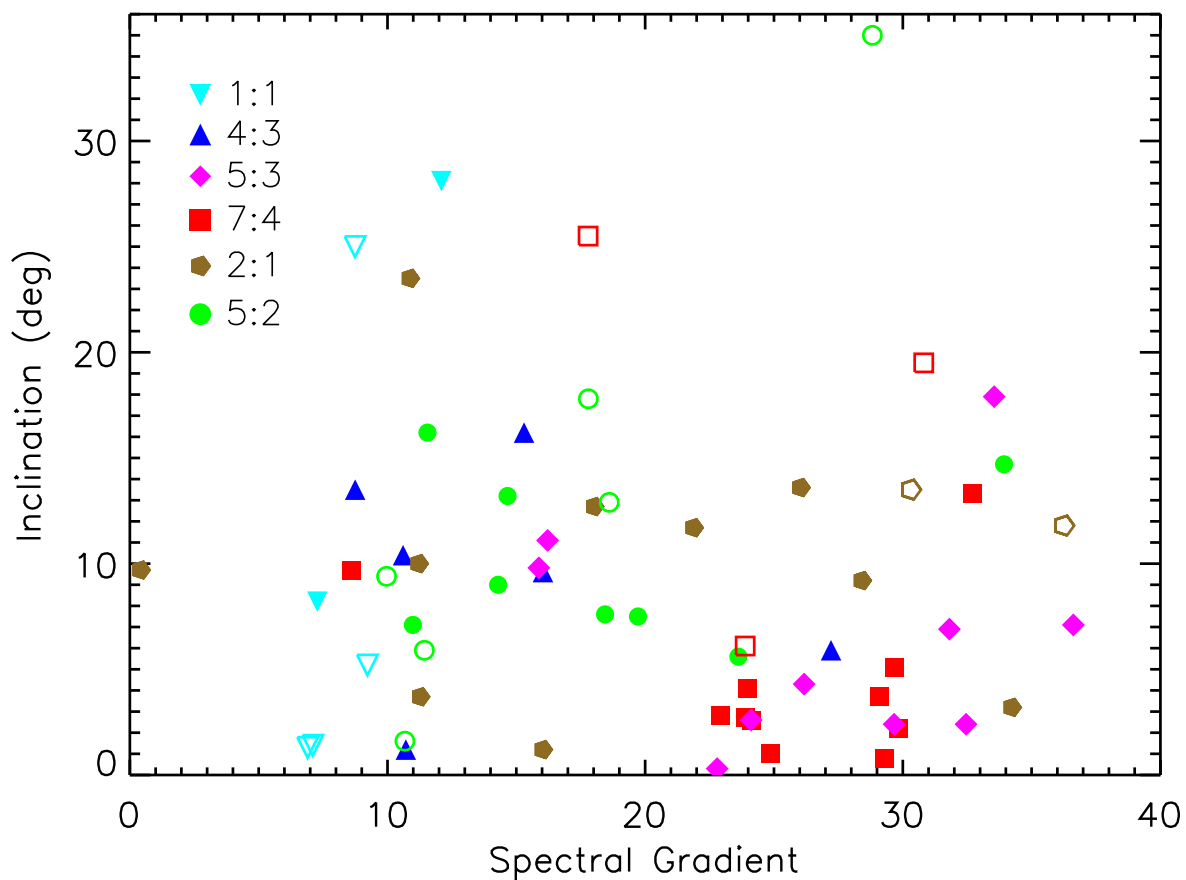


Fig. 7.— Filled symbols show the spectral gradient versus inclination of the main resonances observed in this work. Open symbols show the few measurements found in the literature of resonance objects not observed in this work. There is a lack of low inclination 4:3 objects and high inclination 5:3 and 7:4 objects, but the few observed at these inclinations in these resonances are similar in color as the other objects in the particular resonance. It is interesting that the only non ultra-red objects in the 5:3 and 7:4 resonances have inclinations of about 10 degrees or higher. It is also of note that the only ultra-red object in the 4:3 resonance has an inclination less than 10 degrees. The spectral gradient uncertainties have been removed for clarity but can be found in Table 2.

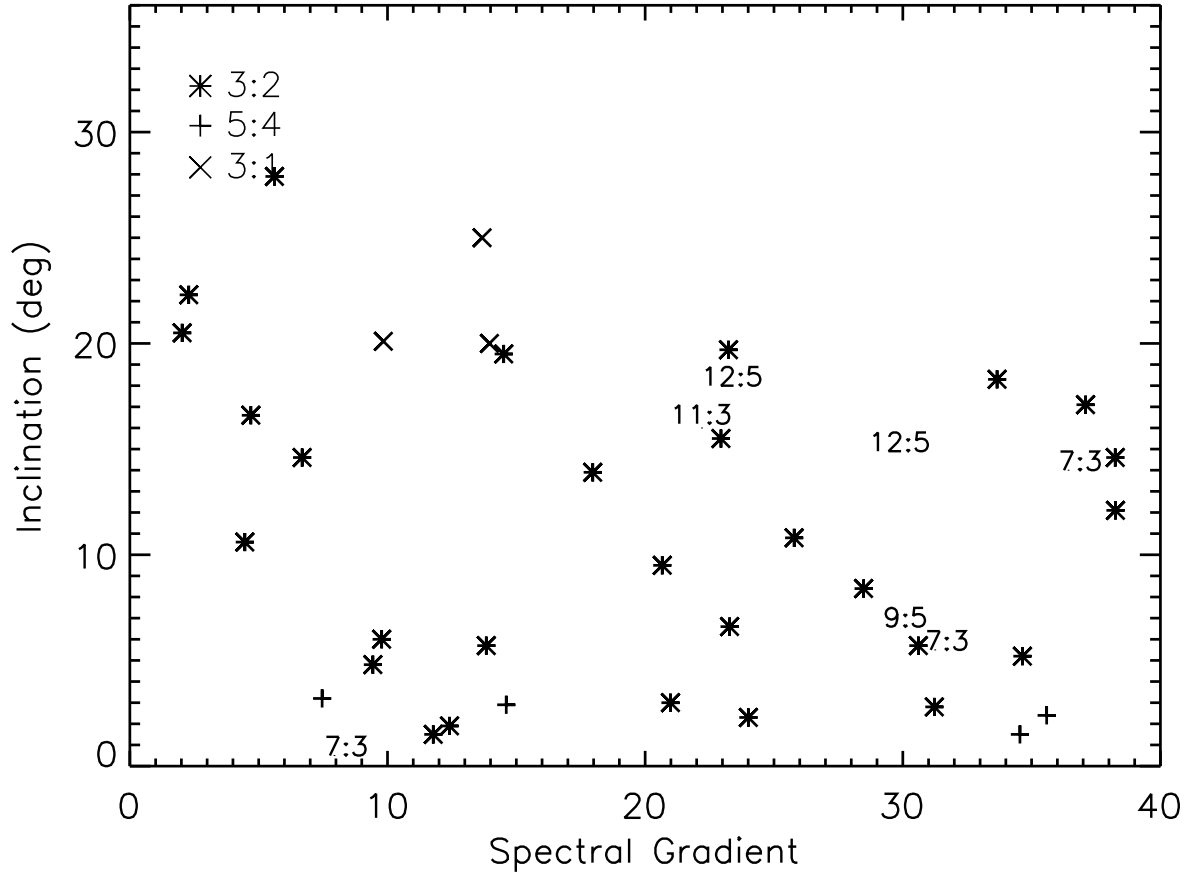


Fig. 8.— The spectral gradient versus inclination of the 3:2 resonance objects and resonances observed with few known members. The 3:2 resonance objects (asterisks) appear to have no color inclination dependence and have a range of colors from neutral to ultra-red. The 5:4 resonance (pluses) has only low inclination members with colors split between moderately red and ultra-red. The 3:1 resonance (crosses) shows only high inclination members with only moderate redness observed for all three objects. The 7:3 resonance has a mix of colors. Resonances with two or less measured members (12:5, 11:3, and 9:5) are shown in the figure by their mean motion resonance ratio relative to Neptune.

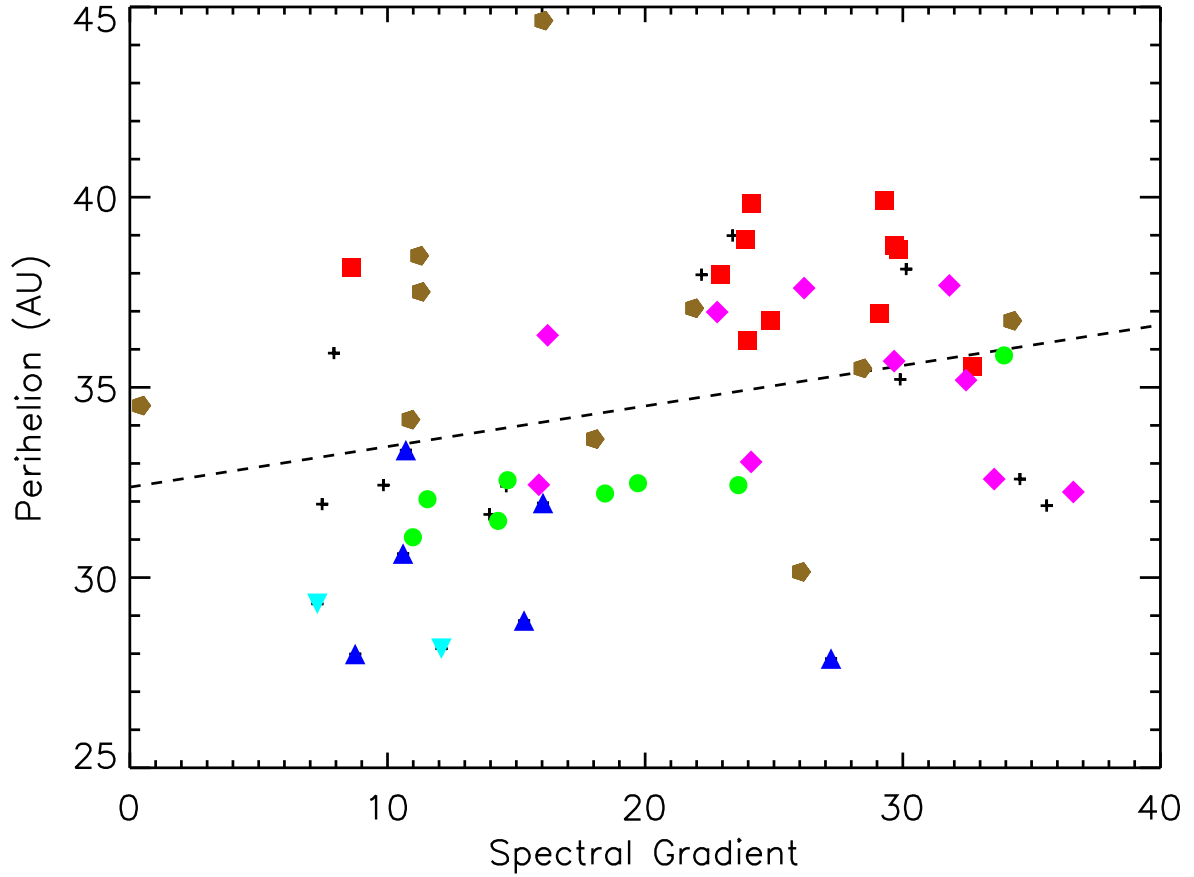


Fig. 9.— Same as Figure 7 except comparing the spectral gradient of the various resonance objects to their perihelion distances. The dashed line is the fit to all the data points. There is a moderate correlation that the higher perihelion objects have redder surfaces, but it is only significant at about the 97% confidence level. The non major less populated resonant objects are shown as plus signs.

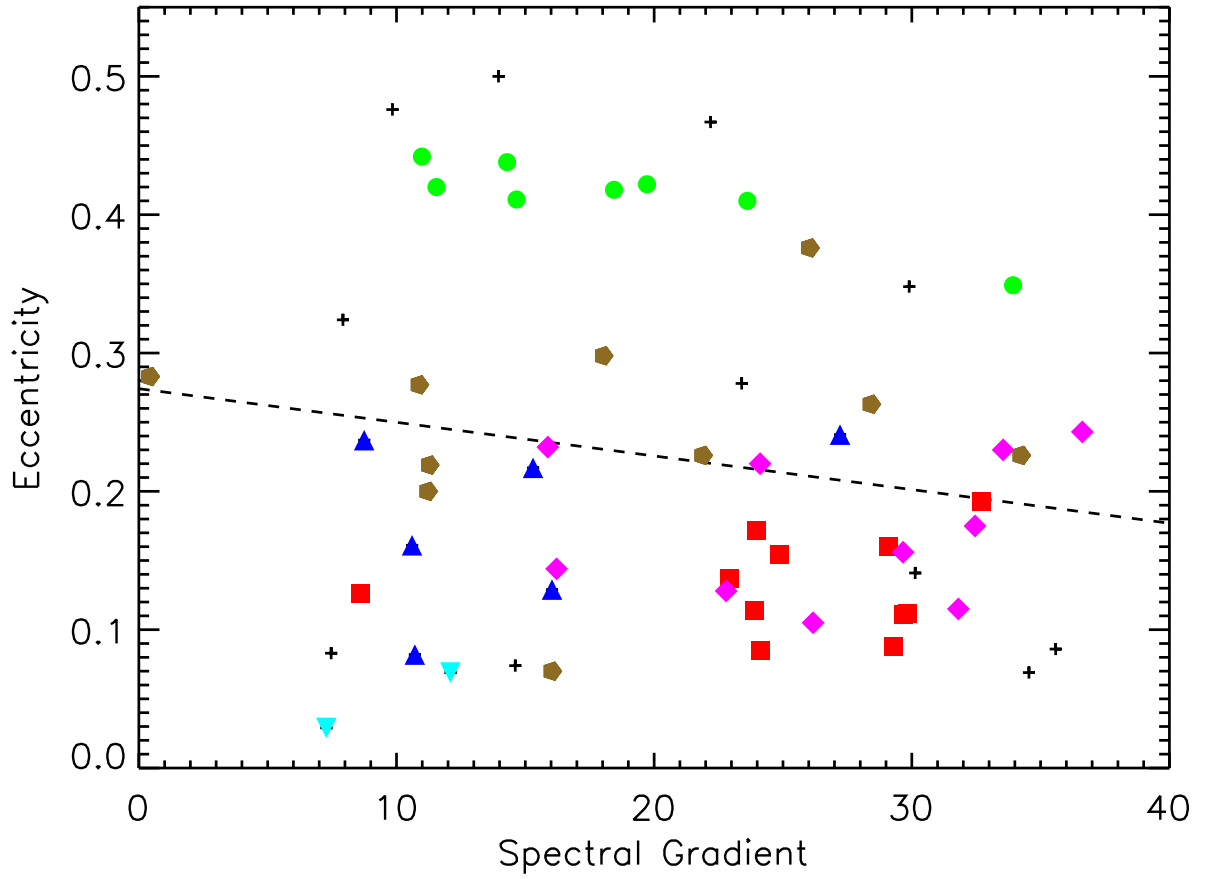


Fig. 10.— Same as Figure 7 except comparing the spectral gradient of the various resonance objects to their eccentricities. There is a slight trend that lower eccentricity objects tend to be redder in color. The non major less populated resonant objects are shown as plus signs.

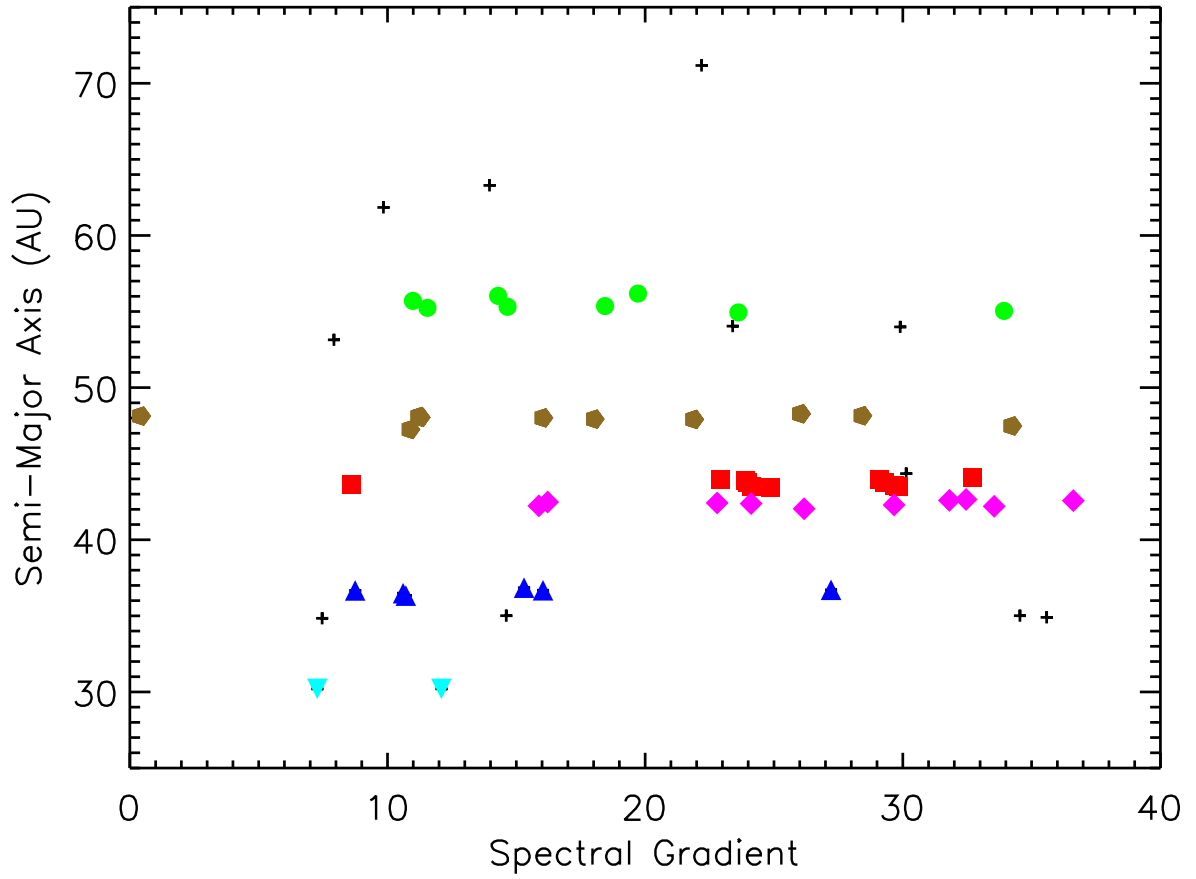


Fig. 11.— Same as Figure 7 except comparing the spectral gradient of the various resonance objects to their semi-major axes. The non major less populated resonant objects are shown as plus signs.

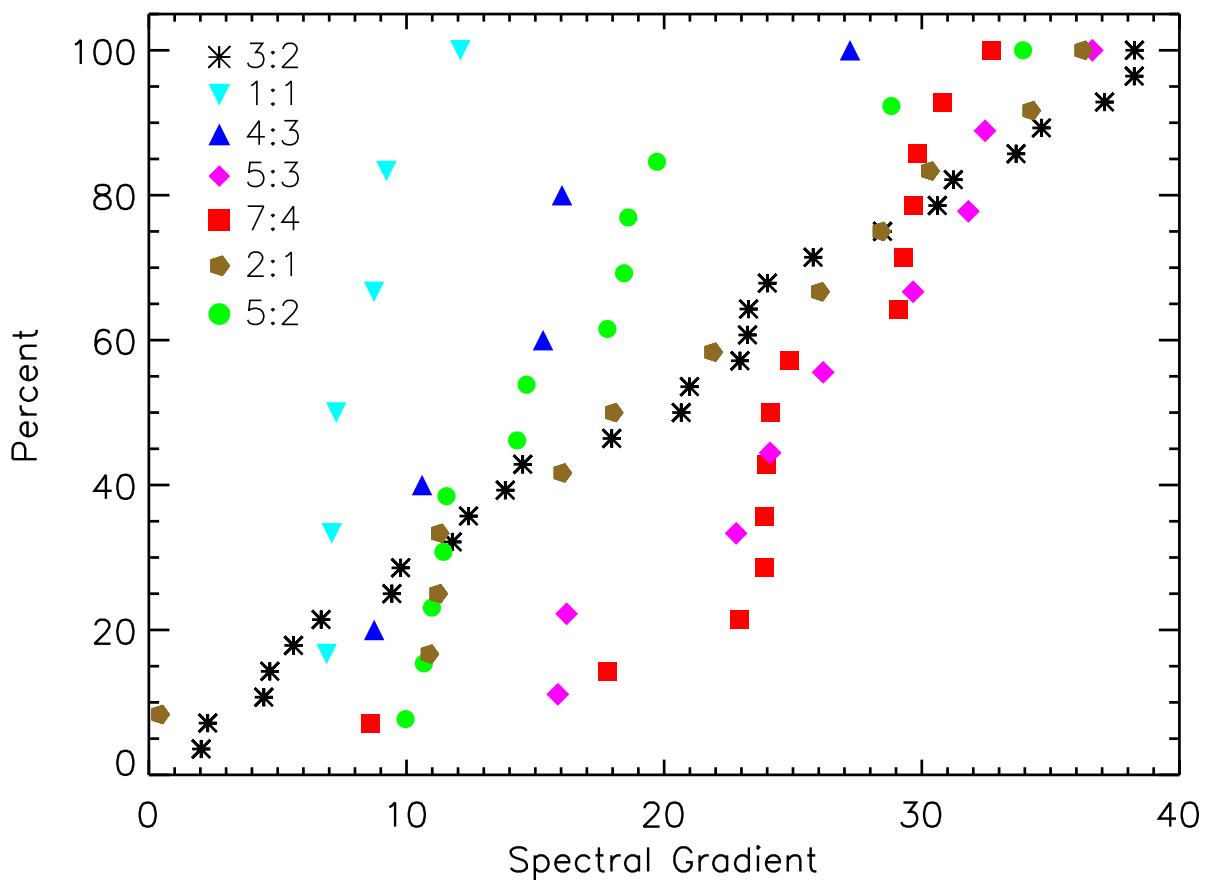


Fig. 12.— The Kolmogorov-Smirnov test (K-S test) plotted for the Neptune Trojans 1:1 (cyan upside down triangles), 4:3 (blue triangles), 5:3 (purple diamonds), 7:4 (red squares), 2:1 (brown pentagons), 5:2 (green circles) and 3:2 (black asterisks). The vertical axis shows the cumulative spectral gradient, S , for the objects, where ultra-red is $S \gtrsim 25$. The Neptune Trojans (1:1) are the most neutral in color and uniform of all the resonances. The 4:3 and 5:2 are mostly only moderately red in color, though the 4:3 resonance has very few low inclination ($i < 10$ deg) objects with measured colors. The 5:3 and 7:4 resonance objects are mostly ultra-red though neither resonance has many high inclination objects with measured colors. The 2:1 and 3:2 resonances seem to have a mix of all object colors and are not dependent on inclination.

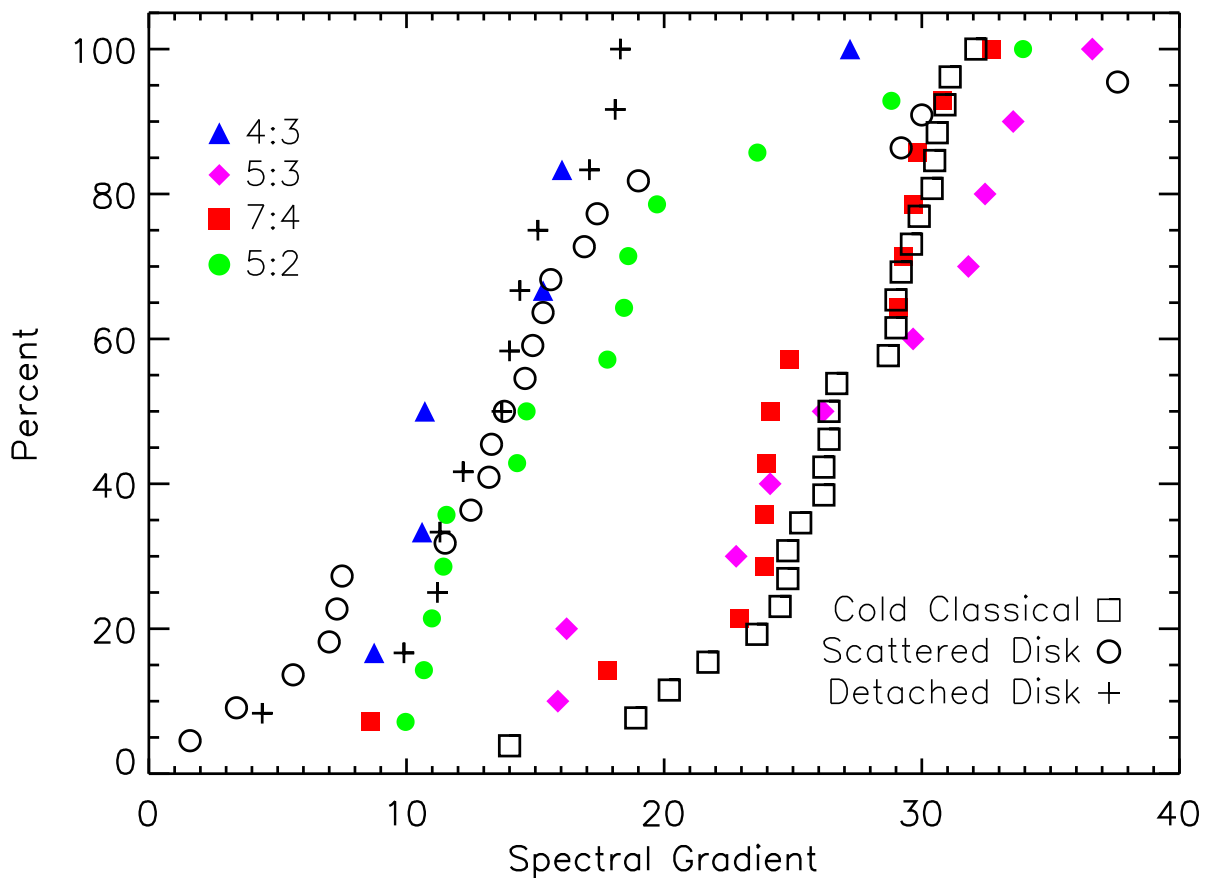


Fig. 13.— Same as Figure 12 except the Scattered Disk (open circles), Detached Disk (pluses), and Cold Classical belt objects (open squares) are shown to compare to the 4:3, 5:3, 7:4 and 5:2 resonances. The 1:1, 3:2 and 2:1 resonances have been removed for clarity. The 4:3 and 5:2 resonances appear to be very similar in color distribution as the scattered disk and detached disk objects while the ultra-red dominated 5:3 and 7:4 resonant populations are very similar in color distribution to the Cold Classical Kuiper belt.